Kisspeptin fiber and receptor distribution analysis suggests its potential role in central sensorial processing and behavioral state control

Running title: Kiss1r and KP fiber mapping in rodent brain

Limei Zhang[1,2,*c], Vito S. Hernández[1,2,*c], Mario A. Zetter[1,5], Oscar R. Hernández-Pérez[1], Rafael Hernández-González[6], Ignacio Camacho-Arroyo[7], Lee E. Eiden[2,c], Robert P. Millar[1,3,4]

[1]Dept. Physiology, School of Medicine, National Autonomous University of Mexico, Mexico City, Mexico
[2]Section on Molecular Neuroscience, NIMH-IRP, NIH, Bethesda, MD, USA
[3]Centre for Neuroendocrinology, University of Pretoria
[4]Dept. of Integrative Biomedical Sciences, Institute of Infectious Disease and Molecular Medicine, University of Cape Town, South Africa
[5]Department of Medicine and Health, University of La Salle, Mexico City, Mexico
[6]Vivarium, School of Medicine, National Autonomous University of Mexico, Mexico City, Mexico
[7]Research Unit in Human Reproduction, National Institute of Perinatology-Faculty of Chemistry, National Autonomous University of Mexico, Mexico City, Mexico
[*]These authors share first authorship.
[c] Correspondence: limei@unam.mx, vitohdez@unam.mx, eidenl@mail.nih.gov

Abstract

Background:
Kisspeptin (KP) signaling in the brain is defined by the anatomical distribution of KP-producing neurons, their fibers, receptors, and connectivity. Technological advances have prompted a re-evaluation of these chemoanatomical aspects, originally studied in the early years after the discovery of KP and its receptor *Kiss1r.* We have previously characterized[(1)] seven KP neuronal populations in the mouse brain at the mRNA level, including two novel populations, and examined their short-term response to gonadectomy.

Methods:
In this study, we mapped KP fiber distribution in rats and mice using immunohistochemistry under intact and short- and long-term post-gonadectomy conditions. *Kiss1r* mRNA expression was examined via RNAscope, in relation to vesicular GABA transporter (*Slc32a1*) in whole mouse brain and to KP and vesicular glutamate transporter 2 (*Kiss1* and *Slc17a6*) in hypothalamic RP3V and arcuate regions.

Results:
We identified KP fibers in 118 brain regions, primarily in extra-hypothalamic areas associated with sensorial processing and behavioral state control. KP-immunoreactive fiber density and distribution were largely unchanged by gonadectomy. *Kiss1r* was expressed prominently in sensorial and state control regions such as septal nuclei, the suprachiasmatic nucleus, locus coeruleus, hippocampal layers, thalamic nuclei, and cerebellar structures. Co-expression of *Kiss1r* and *Kiss1* was observed in hypothalamic neurons, suggesting both autocrine and paracrine KP signaling mechanisms.

Conclusion:
These findings enhance our understanding of KP signaling beyond reproductive functions, particularly in sensorial and behavioral state regulation. This study opens new avenues for investigating KP's role in controlling complex physiological processes, including those not related to reproduction.

key words*: behavior state system, sensorial-motor circuits, extrahypothalamic kisspeptin signaling, Kiss1r, autocrine*

1. Introduction

Kisspeptin (KP) is a neuropeptide encoded by the *Kiss1* gene, initially known as metastin, and identified for its activity in inhibiting cancer metastasis[2]. It is now well-recognized as a critical regulator of the mammalian reproductive system, playing a pivotal role in the activation of the hypothalamo-pituitary-gonadal (HPG) axis by stimulating the release of gonadotropin-releasing hormone (GnRH)[3, 4]. Beyond its reproductive functions, KP is increasingly implicated in a variety of physiological processes, including the regulation of emotions and cognitive functions[5], especially, although not limited to, those involved in sexual behavior[6]. For instance, kisspeptin receptors are expressed in the amygdala and hippocampus, critical regions for emotional processing, and have been associated with anxiolytic/anxiogenic effects and the modulation of stress[7-9] and fear responses[10-12]. Additionally, KP has been implicated in cognitive functions such as learning and memory, potentially through its actions within the hippocampus and prefrontal cortex[13]. Thus, KP is likely to play a multifaceted role in brain function, beyond control of the HPG axis.

In a recent study in mouse, our group reported a comprehensive KP cell population description and molecular signature characterization within the excitatory/inhibitory (glutamatergic-GABAergic) context throughout mouse brain, using a sensitive dual and multiple channel in situ hybridization method. We described chemotypes of seven distinct KP populations, four of them within the hypothalamus and three of them as extrahypothalamic populations. The KP cell groups located in the ventral division of the premammillary nucleus of the hypothalamus and the nucleus of tractus solitarii in the brain stem, are new additions to the literature. Their up- and down regulation by short-term gonadectomy (GNX) was also reported quantitatively[1]. These results prompted us to extend the study by focusing on kisspeptin immunopositive fiber-distribution in both rat and mouse, and on rodent KP receptor (*Kiss1r*) distribution using the RNAscope method.

There had been comprehensive anatomical studies on KP neuronal populations and fiber distributions in the brain of diverse animal species in the literature of the first decade after the discovery of KP, albeit hypothalamic, rather than extrahypothalamic regions, were the main focus of those studies due to the role of KP in HPG axis regulation[13-18]. However, KP may also regulate sexual behavior, in additional to reproductive endocrinology, within the mammalian brain[6]. Due to the emerging evidence for kisspeptin function beyond its well-documented role in orchestration of GnRH secretion in the hypothalamus, more comprehensive data on the distribution of kisspeptin cell bodies and nerve fibers throughout the brain are needed. In particular, some data have been questioned as potentially unreliable, due to possible adventitious cross-reactivity with other RFamide-peptides[16]. We have used a KP antibody with well-documented authenticity and lack of cross-reactivity, and applied state-of-the-art tissue preparation and staining methods [19] in this study. Providing a reliable and comprehensive description of the distribution of KP cell bodies and fibers throughout the brain should contribute to a better understanding of the possible role(s) of KP first messenger function relevant to both reproductive and non-reproductive behavior. We report here 118 brain regions that contain KP fibers and terminals, with most of them located in extra-hypothalamic regions closely involved in central sensorial processing and behavioral state control[20-25]. KP fiber density was similar in long-term (one year) gonadectomized compared to intact male or female mice.

The kisspeptin receptor (Kiss1R), was first identified in rat in 1999 as an orphan receptor previously called Gpr54[26]. Kiss1R is a metabotropic receptor coupled to Gq/11, and its inactivation has been associated with hypogonadism[27]. After KP binds its receptor, phospholipase C (PLC) is activated and hydrolyzes phosphatidylinositol 4,5-bisphosphate (PIP2) to produce diacylglycerol (DAG) and inositol 1,4,5-trisphosphate (IP3) with a rise in Ca++ mobilized from intracellular stores and the activation of protein kinase C (PKC)[28, 29]. There have been few reports on Kiss1R expression in the CNS[27, 28, 30, 31] and a comprehensive description, especially Kiss1R co-expression within the context of excitatory and inhibitory neurotransmission, is incomplete. In this study, we used the RNAscope dual and multiplex in situ hybridization method to map the Kiss1r expression throughout mouse brain. *Kiss1r* was prominently expressed in brain sensory and state control regions, such as main and accessory olfactory bulbs, septal nuclei, tuberomammillary nuclei, the suprachiasmatic nucleus, the locus coeruleus, the hippocampal pyramidal and granule cell layers, the thalamic nuclei, and the cerebellar granule cell layer, as well as the interposed nucleus. *Kiss1r* was also co-expressed in *Kiss1*-expressing hypothalamic neurons and neighboring cells, suggesting the KP system uses autocrine and paracrine mechanisms. Data from this study provide additional anatomical features of the KP system for further hypothesis generation and testing of the role of KP beyond HPG axis regulation.

2. Material and methods

2.1. Animals

Wistar rats (N=12, male = 6, female = 6) and C57BL/6 mice (N=30, male = 15, female = 15) were obtained from the local animal vivarium and housed three per cage under controlled temperature and illumination (12h/12h) with water and food *ad libitum*. Mice subjected to gonadectomy were singly housed for recovery for one week after surgery and then returned to their home cages. All animal procedures were approved by the local research ethics supervision commissions (license number CIEFM-079-2020, UNAM and NIMH/ACUC approval LCMR-08).

To evaluate the effect of gonadectomy on the expression of kisspeptin throughout the brain in male and female mice, we compared the KP immunoactivity of 24 mice distributed in the following experimental groups:

Male				Female			
Five month old		Fifteen month old		Five month old		Fifteen month old	
Intact	1 mo ORX	Intact	12 mo ORX	Intact	1 mo OVX	Intact	12 mo OVX
n=3	n=3	n=3	n=3	n=3	n=3	n=3	n=3

For RNAscope ISH experiments, we used three male and three female mice of three months of age. Vaginal cytology was performed in female mice to assess the estrous cycle. Brains were collected during the proestrus stage associated with a high level of estrogen.

2.2. Gonadectomy

133 *2.2.1 Mouse ovariectomy (OVX)*
134
135 A dorsal approach to remove the ovaries was used [32]. Briefly, animals were anaesthetized with ketamine
136 90 mg/kg + xylazine 20 mg/kg *i.p.* Under anesthesia, animals were placed in ventral recumbency and a 3
137 cm/side square region centered over the third lumbar vertebra shaved. The shaved area was disinfected
138 with Povidone and 70% alcohol, and a sterile fenestrate drape was placed over it. A single midline dorsal
139 incision approximately 1 cm long was made in the skin at the level of the bottom of the rib cage. The
140 incision was moved laterally to cut the right and left abdominal walls. After cutting the wall (oblique and
141 transverse abdominal muscles), blunt dissection through the body wall with mosquito hemostats was
142 performed. Forceps were gently and carefully introduced to retrieve and exteriorize the ovary. The ovary,
143 ovarian vessels, and ligament were ligated with 4-0 synthetic absorbable sutures and cut. The wall muscle
144 layer incision was closed with a 4-0 synthetic, monofilament, absorbable suture. The skin incision was
145 closed with a subcuticular suture.
146
147 *2.2.2 Mouse orchiectomy (ORX)*
148
149 For the excision of the testicles, we followed a midline incision technique[33]. Briefly, animals were
150 anaesthetized with ketamine 75 mg/kg + xylazine 16 mg/kg i.p. and placed on the operating table on their
151 backs. The central ventral side of the scrotum area was disinfected with Povidone and 70% alcohol. A
152 single incision on the ventral side of the scrotum (1 cm long) penetrating the skin was performed. Each
153 cremaster muscle was cut, and each testis was exposed by gently pulling it through the incision using blunt
154 forceps. Cauda of the epididymis, caput epididymis, vas deferens, and testicular blood vessels were
155 exposed while holding the testicular sac with sterile tooth forceps. A single ligature 4-0 synthetic
156 absorbable suture around the vas deferens and blood vessels was made, prior to excision and gentle
157 removal of the testis. The remaining content was replaced in each one of the testicular sacs. The skin
158 incision was closed with a subcuticular suture.
159
160 <u>2.3 Immunohistochemistry (IHC)</u>
161
162 Animals were deeply anaesthetized with sodium pentobarbital (100 mg/kg, *i.p.*). They were perfused
163 transaortically with 0.9% saline followed by a cold fixative containing 4% paraformaldehyde in 0.1 M
164 sodium phosphate buffer (PB, pH 7.4) plus 15% v/v saturated picric acid for 15 min. Brain tissues were
165 rinsed immediately after the 15 min fixation, until the buffer was colorless. Brains were then sectioned
166 the same day, using a Leica VT 1000S vibratome at 70 µm thickness, in the coronal and parasagittal planes,
167 and the immunohistochemical (IHC) reaction was performed the same day. This procedure yielded a more
168 comprehensive IHC labelling than longer fixation and delayed IHC as previously reported and
169 discussed[19]. One of every three sections was selected, and sections from animals that would be compared
170 (*i.e.*, female control *vs.* female gonadectomy) were incubated in the same vial. To block the unspecific
171 antibody binding, sections were incubated for one hour in a solution consisting of 20% normal donkey
172 serum (NDS) diluted in Tris-buffered saline (TBS, pH 7.4) plus 0.3% Triton-X (TBST). After the blocking
173 step, sections were incubated for 48 h at 4ºC in a polyclonal sheep anti-kisspeptin antibody[34] (GQ2,
174 kindly supplied by Mohammad Ghatei†, Imperial College, London, UK), diluted at a 1:5000 concentration
175 in TBST + 1% NDS. This antibody recognizes kisspeptins 54, 14, 13, and 10 that conserve the C-terminal

176 decapeptide essential for biological activity and shows virtually no cross-reactivity (<0.01%) with other
177 related human RF-amide peptides[34]. After three wash steps, sections were incubated for 24 h with the
178 secondary donkey anti-sheep biotinylated antibody (Cat: 713-065-147, Jackson ImmunoResearch Inc, PA,
179 USA) diluted at a concentration of 1:500 in TBST + 1% NDS. To detect the biotinylated antibody,
180 VECTASTAIN Elite ABC HRP Kit (Cat: PK-6100, Vector Laboratories, Inc. CA, USA) was used, with
181 H_2O_2 and 3,3'-diaminobenzidine as substrates. Finally, sections were mounted on glass slides, dehydrated,
182 dipped in xylene, and cover-slipped using Permount™ mounting medium.
183

184 2.4 Anatomical assessment of kisspeptin innervation density and comparison between control and
185 gonadectomized animals
186

187 To assess the projection patterns of kisspeptin immunopositive fibers throughout the brain four
188 researchers independently examined the slides under a light microscope, after identifying the regions
189 based on the Paxinos Rat & Mouse brain atlases[35, 36]. Scores of "+" (sparse, main axons passing, without
190 branching nor axon terminals); "++", scattered, some branching; "+++", moderate, abundant branching
191 and axon terminals; "++++", intense, extensive branching and intense axon terminals, with confluent
192 fibers that it was difficult to see a separation between them, were reported.
193

194 2.5 Anatomical assessment of *Kiss1r* mRNA expression in the context of Slc32a1-expressing neurons
195 throughout the brain
196

197 Six C57Bl mice, 3 male and 3 female of 12-14 weeks old, were deeply anesthetized with sodium
198 pentobarbital (100 mg/kg b.w., i.p.) and decapitated using a small animal guillotine. The brains were then
199 extracted and rapidly frozen in Dry Ice. Fresh-frozen brains were sectioned sagittally into 12 µm thick
200 slices using a Leica CM-1520 cryostat and mounted onto positively charged Superfrost Plus microscope
201 slides (Cat. 22-037-246, Fisher Scientific, Pittsburgh, PA). The detailed methods have been previously
202 described [1, 37, 38].
203

204 Probes used for the detection of mRNAs in the double or multi-channel *in situ* hybridization (DISH
205 and MISH) were custom-designed by Advanced Cell Diagnostics (https://acdbio.com/rnascope-25-hd-
206 duplex-assay) for kisspeptin (Mm-Kiss1, channel 1 probe), VGAT (Mm-Slc32a1, channel 1 and channel
207 4 probes), kisspeptin receptor (Mm-Kiss1r, channel 2 probe) and VGLUT2 (mm-*Slc17a6*, channel 3). All
208 experimental procedures were carried out in accordance with the manufacturer's protocol. After sectioning,
209 the slides were fixed in chilled 4% paraformaldehyde (Cat. 30525-89-4, Sigma-Aldrich) prepared in
210 phosphate-buffered saline (Cat. M32631, Sigma-Aldrich), dehydrated in ethanol, and treated with
211 hydrogen peroxide for 15 minutes. They were then treated with protease III for 20 minutes at room
212 temperature, incubated for two hours with the probe mixtures, and underwent amplification and detection
213 steps following the manufacturer's guidelines. Finally, the slides were counterstained with hematoxylin in
214 case of DISH and cover-slipped.
215

216 The processed sections were examined using a Nikon Eclipse E600 microscope along with its
217 digital camera for photographic documentation. Multichannel in situ hybridization (ISH) sections were

analyzed using the Stellaris Confocal Microscope from Leica Microsystems. Sections were subsequently scanned using the ZEISS Axio ScanZ.1.

For the semi-quantitative analysis, we determined the percentage of *Kiss1r*-labeled cells that co-expressed *Slc32a1* for the column titled 'Slc32a1 co-expression' and the total number of Nissl-labeled nuclei (NLN) versus Kiss1r on NLN without Slc32a1 labeling for the column titled 'No Slc32a1 co-expression' for each region of interest. The number of "+" assigned was based on the following criteria: if the percentage fell within the ranges of 1% to 20% it was assigned (+); from 21% to 40%, (++); from 41% to 60%, (+++); from 61% to 80%, (++++); and from 81% to 100%, (+++++).

3. Results and focused discussion

3.1 Regional distribution of kisspeptin-expressing fibers and neurons in the mouse and rat brain

In Table 1, we report 118 regions of the rodent brain where we observed kisspeptin (KP immunoreactivity (ir) with varying strengths. We identified only one previous anatomical mapping study on the distribution of KP immunoreactivity in the rat brain that had a similar level of completeness compared to our data. In that study, the authors utilized an antibody produced by Phoenix Pharmaceuticals [39], which has been noted as potentially cross-reactive with other RFamide-related peptides[16]. We included the data reported by Brailoiu et al.[39] in rat, using the Phoenix Pharmaceuticals antibody anti-metastin (MT), in the Table 1, highlighted in blue to facilitate comparison with our current findings. All the regions reported in this earlier study were replicated in our experiments, which suggests that the value of the earlier report may have been underestimated. Furthermore, we identified numerous additional regions containing KP-expressing fibers.

The rat brain, particularly in telencephalic regions (*vide infra*), exhibited stronger immunohistochemical labeling for KP than the mouse brain. However, quantitative conclusions cannot be drawn confidently due to variability among experimental subjects and immunoreactions. Sex differences in the distribution of cells or fibers were inconsistent among experimental subjects, even under identical experimental procedures. For example, within a given region, some reactions were stronger than others, and these differences were not consistently associated with sex or treatment of the subjects. Various unknown factors may have influenced these observations. It is important to note that KP expression may be up- or down-regulated in individual organisms due to their physiological regulation, affecting the presence or absence of peptide vesicles at a given location at the time of perfusion-fixation. Specifically, a kisspeptinergic cell (referring to a neuron that can synthesize Kp and transport it to its axon or dendrite) can only be detected with KP-IHC if the segment is filled with peptidergic vesicles at the moment of fixation. However, determining these factors falls outside the objective of our study, which aims to qualitatively determine the Kp signaling beyond reproductive functions, especially in the brain regions implied to sensory and behavioral states. Based on these observations and rationale, we pooled data from male and female subjects for Table 1 and Figures 1-3, while separating the observations by rodent species (i.e., mouse in Figures 1 and 2 versus rat in Figure 3) to depict the highest possible KP expression in a given region as representative of "ideal subjects." This scoring reflects the maximum density observed for each region, providing insight into the maximum potential expression of KP in living rodents. In

Supplementary Information (SI) Figure 1, we present examples of KP IHC labeling in young male and female mice, both intact and gonadectomized, to further illustrate this point.

Table 1. Comparison of the distribution of kisspeptin immunoreactive fibers in mouse and rat brain using antibody GQ2 (current study) to earlier reports using metastin MT antibody (Brailoiu et al, JCN, 2005)

Structure	Abbr.	irMT cells (rat)	irGQ2 cells rat	irGQ2 cells mouse	irMT fibers (rat)	irGQ2 fiber rat	irGQ2 fiber mouse	Axons from RP3V viral tracers	Axons from Arc viral tracers
Telencephalon									
Cerebral cortex									
Cingular cortex	Cg		-	-		++	+		
Dorsal peduncular cortex	DP		-	-		++	+		
Dorsal tenia tecta	DTT		-	-		++	+	+	
Infralimbic cortex	IL		-	-		++	+		
Prelimbic cortex	PrL		-	-		++	+		
Ventral orbital cortex	VO		-	-		++	+		
Olfactory area									
Anterior olfactory nucleus	AON		-	-		++	-		+
Olfactory tubercle	Tu		-	-		++	-		
Extended amygdala									
Anterior amygdala	AA		-	-		++	+		
Bed nucleus of stria terminalis medioanterior	BSTMA		-	-	++	+++	+++		+
Bed nucleus of stria terminalis medioposterior	BSTMP		-	-	++	+++	+++		+
Bed nucleus of stria terminalis laterodorsal (oval)	BSTLD		-	-	++	+	+	++	
Bed nucleus of stria terminalis lateroventral	BSTLV		-	-	++	+++	+++	++	
Bed nucleus of stria terminalis lateroposterior	BSTLP		-	-	++	+++	+++		
Basolateral amygdala	BLA		-	-	+	+	+		
Basomedial amygdala	BMA		-	-	+	+	+	++	+
Bed nucleus of stria terminalis intra-amygdala division	BSTIA		-	-		++	++		
Central amygdaloid nucleus, lateral	CeL		-	-	+	+	+	-	-
Central amygdaloid nucleus, capsular	CeC		-	-		++	++	-	-
Central amygdaloid nucleus, medial	CeM		-	-	+	++	++	-	-
Cortico-amygdala	CoA		-	-		+	+		+
Medial amygdaloid nucleus, posterodorsal	MePD		+	+		++	++		+
Medial amygdaloid nucleus, posteroventral	MePV		-	-		++	++	+	+
N. lat. olfactory tract	NLOT		-	-		+	+	-	
Stria terminalis	st		-	-		+	+		
Basal ganglia									
Accumbens n., core	AcbC		-	-	+	++	++	+	+
Accumbens n., shell	AcbSh		-	-		+++	++	++	+
Caudate putamen	CPu		-	-	+	+	+		
Globus pallidus	GP		-	-		+	+		
Internal capsule	ic		-	-		+	+		
External capsule	ec		-	-		+	-		
Substantia innominata	SI		-	-		+	+	+	
Ventral pallidum	VP		-	-	+	++	++		
Septum									
Lat. septal n. dorsal	LSD		-	-	++	+++	+++	+	

Lat. septal n. int	LSI		-	-	+	+	+		++
Lat. septal n. ventral	LSV		-	-	++	+++	+++	+++	++
Medial septal nucleus	MS		-	-	+	+++	+	+	+
Septo-fimbrial n.	SFi		+	+		+	+	++	
Septo-hippocampal n.	SHi		+	+		+	+		
N. horizontal limb of the diagonal band	HDB		-	-	+	+	+	++	+
N. vertical limb of the diagonal band	VDB		-	-	+/-	+	+	+++	+
Diencephalon									
Hypothalamus									
Anteroventral periventricular n.	AVPe		+++	+++		+++	+++	+++	+++
Rostral periventricular area	RP3V		+++	+++		+++	+++		
Anterior hypothalamic area anterior	AHA		-	-		++	++	++	+++
Anterior hypothalamic area posterior	AHp		+	+	+	++	++		+++
Arcuate nucleus	Arc	+	++	++	+++	++++	++++	+++	++++
Dorsal hypothalamic	DH		+	+	+	+	+	+++	
Dorsomedial hypothalamic area	DM	+++	++	++	++	++	++	+++	++
Lat. hypothalamic area	LH		-	-	+	+	+	+	+
Lat. preoptic area	LPO		-	-	+	++	++	+++	
Medial preoptic area	MPA		-	-	+	++	++	+++	++
Medial preoptic n.	MnPO		-	-	+	+++	+++	++++	+++
Parastrial nucleus	PS		-	-	+++	+++	+++		
Paraventricular hypothalamic n.	PVN	+	-	-	+	++	+	+++	+
Paraventricular hypothalamic n. medial magnocellular div	PVNmm		-	-		+++	+++	+++	+
Pa hypothalamic n. lateral magnocellular div.	PVNlm		-	-		+	+	+++	+
Pa hypothalamic n. medial parvocellular div.	PVNmp		-	-		+++	+++	++	
Periventricular hypothalamic n. anterior	PVa		-	-		++	++		+++
Premammillary n. ventral	PMv		+	+		+++	++	+++	+++
Posterior hypothalamic area	PH		-	-	+	+	+	++	++
Retrochiasmatic area	RCh		-	-	+	+	+	++	++
Supraoptic nucleus	SON		-	-	+	++	++	+	
Tuber cinereum area	TC		-	-	+	++	+	++	
Ventral tuberomammillar n.	TMv		-	-		+++	++		+++
Ventromedial hypothalamic nucleus	VMH	+	-	-	+	+	+		+
Thalamus									
Anteromedial thalamic nucleus	AM		-	-		++	++		
Central medial thalamic nucleus	CM		-	-	+	+	+	++	
Mediodorsal thalamic nucleus	IMD		-	-	+	+	+		
Paratenial thalamic nucleus	PT		-	-	+	+	+		
Periventricular thalamic nucleus	PVT		-	-	+++	++++	++++	++	+
Reuniens thalamic nucleus	Re		-	-	+	+	+		
Rhomboid thalamic nucleus	Rh		-	-	+	+	+		
Submedius thalamic nucleus	SubD		-	-		+	+		
Zona incerta	ZI		-	-	+	+	+		
Epithalamus									
Habenular nucleus	Hb		-	-	++	++	++	+	
Mesencephalon									
Central nucleus of the inferior colliculus	CIC		-	-	+	++	++		
Cuneiform nucleus, dorsal part	CnFD		-	-		++	++		
Dorsal raphe nucleus	DR		-	-	+	++	++		
Deep mesenceph. n.	DpMe		-	-	+	+	+		

Interpeduncular n.	IP		-	-		+	+		
Median raphe n.	MnR		-	-	+	+	+		
Periaqueductal gray, lateral	LPAG		-	-		++	++	++	+
Periaqueductal gray dorsomedial	DMPAG	+/-	-	-	+++	+++	+++	++	+
Substantia nigra	SN		-	-	+	+	+		
Superior colliculus, intermediate and deep gray layer	DpG		-	-	+	+	+		
Supramammilary n.	SuM		-	-	+	+	++		
Ventral tegmental area	VTA		-	-		+	+	+	
Metencephalon and myelencephalon									
Ambiguus nucleus	Amb		-	-	+	+	+		
Area postrema	AP		+	+		+++	+++		
Caudoventrolateral reticular nucleus	CVL	+	-	-	+	++	++		
Dorsomedial tegmental area	DMTg		-	-		+	+		
Gigantocellular reticular nucleus	Gi		-	-	+	++	++		
Intermediate reticular nucleus	IRt		-	-	++	++	++		
Lateral parabrachial nucleus	LPB		-	-	+++	++++	++++	+	
Lateral reticular nucleus	LRt	+			++	++	++		
Lateral superior olive	LSO		-	-	++	+	+		
Locus coeruleus	LC		-	-	++	+++	+++	+	
Medial vestibular nucleus, magnocellular part	MVeMC		-	-	.	++	++		
Medioventral periolivary nucleus	MVPO		-	-		+++	+++		
Medullary reticular nucleus, dorsal part	MdD		-	-	+	++	++		
Medullary reticular nucleus, ventral part	MdV		-	-	+	+	+		
Nucleus of the solitary tract	Sol	+++	++	++	+++	++++	++++		
Parvicellular reticular nucleus	PCRt		-	-		++	++		
Parabrachial pigmented nucleus	PBP		-	-		+	+		
Pontine nuclei	Pn		-	-	+	-	-		
Pontine n, brachium pontis	bpPn		-	-		+	+		
Pontine raphe nucleus	PnR		-	-	+	-	-	+	
Pontine reticular nucleus, caudal part	PnC		-	-	+	+	+	++	
Pontine reticular nucleus, oral part	PnO		-	-	+	+	+	++	
Principal sensorial 5 n. dorsomedial	Pr5DM		-	-		++++	++++		
Raphe magnus nucleus	RMg		-	-	+	+	+		
Raphe obscurus nucleus	Rob		-	-	+	+	+		
Raphe pallidus nucleus	RPa		-	-	+	+	+		
Rostroventrolateral reticular nucleus	RVL	-	-	-	++	++	+		
Rubrospinal tract	rs	-	-	-	++	++	++		
Spinal trigeminal tract	Sp5	+	-	-	+++	-	-		
Spinal 5, gelatinous layer	Ge5		-	-		++++	+		
Superior cerebellar peduncle	scp		-	-		+++	+++		

Table caption: Distribution of kisspeptin immunoreactive (antibody GQ2) fiber distribution in mouse & rat brain with comparison of metastin, MT from Brailoiu et al, JCN, 2005 [39] in blue lettering. Semiquantitative annotations are used here: "-", not detectable; "+", weak; "++", low; "+++", moderate; "++++", intense; "+++++", very intense. Anatomical regions are ordered based on Brailoiu et al, JCN, 2005 modified based on Allen Institute Mouse Reference Atlas. Regions of rat brain with higher density of KP fibers are highlighted with bold lettering. The two columns to the right are from analysis of two Kiss1-Cre mice injected Cre-dependent tracer in the arcuate nucleus (Arc, experiments

232311236 and 232310521) and two in the rostral periventricular region (R3PV, experiments 299247009 and 301989585) from the Allen Mouse Brain Connectivity Atlas (https://connectivity.brain-map.org/).

In Figure 1, we show KP immunohistochemical reactivity (-ir) in regions, including anteroventral periventricular nucleus (AVPV) and ventromedial preoptic area (VMPO), where KP functions to regulate GnRH secretion, in comparison with other brain regions, with equally intense KP innervation, that are relevant to regulation of dan yang

, including median preoptic nucleus (MnPO), septohypothalamic nucleus (SHy), medial septal nucleus (MS, panel A2), lateral septal nucleus (LS) and bed nucleus of stria terminalis (BST, which includes the medioanterior, medioventral and lateroventral divisions, STMA, STMV and STLV, respectively) (panel A). In panel A3, KP-ir cell bodies can be seen in the periventricular region (black arrows). Numerous KP-ir fibers are densely distributed at the ventricular wall with several endings observed at the ventricular lining within the ependymal cell layer (red arrows), suggesting a humoral-secretory function of KP signaling. Panel B depicts a coronal section around Bregma -0.15mm, where four main conducting fiber systems can be clearly seen, i.e. the anterior commissure (ac), the stria medullaris (sm), the stria terminalis (st) and the fornix (f). KP-ir fibers running inside these conducting systems are indicated with red arrows. The dense innervation pattern of KP-ir fibers in the paraventricular anterior nucleus of the thalamus is shown (panel B). In panels C and D we show examples of KP-ir cell bodies and fibers in amygdalar complex. KP-ir fibers can be seen inside the stria terminalis (st), bed nucleus of stria terminalis, intra-amygdalar division (STIA), baso-medial amygdala (BMA), nu. basalis of Meynert (NBM) and medial amygdala (MEA). Interestingly, some fibers within the medial amygdala, postero-dorsal division (MEApd), are observed coming from the stria terminalis, with main axons branching within the MEApd, and possibly originating from the hypothalamus. We observed fibers reaching to amygdala, through the stria terminalis (C1, red arrows). This observation is also supported by the analysis from the Allen Mouse Brain Connectivity Atlas (see Table 1, last two columns entitled "Axons from RP3V viral tracers" and "Axons from Arc viral tracers" and in the SI Figure 2). Panels E and F show the microphotographs taken from the hypothalamic tuberal region, where the KP-ir cell bodies are seen in the posterior division of the arcuate nucleus (ArcP), in premammillary nucleus, ventral division (PMv). KP-ir fibers are observed in other regions relevant for behavioral state control at this level, such as ventral tuberomammillary nu (TMv), magnocelular tuberomammillar nu. and dorsal tubero-mammillary nu., posterior hypothalamus, zona incerta (ZI) and subthalamic nu. (STN) (E). E2 shows the third ventricle at the level of Arc posterior. Abundant KP-ir fibers extended toward the lumen of the ventricle (also see A3, red arrows). Panel G-K are micrographs of samples from parasagittal sections of mouse hindbrain. G shows the KP-ir cell bodies and dense KP-ir fibers in the solitary tract (sol) nu. (NTS) of mouse medulla. H and I show the dense innervation pattern of KP-ir fibers in pontine nuclei: lateral parabrachial nu. (LPBN) and locus coeruleus (LC) respectively. J and K show the dense KP-ir fibers in the spinal trigeminal tract (Sp5, K) and in the gelatinous layer of Sp5 (Ge5). Note that within the Ge5, the KP-ir fiber make perisomatic contacts with the cell bodies of the Ge5 (J, red arrows).

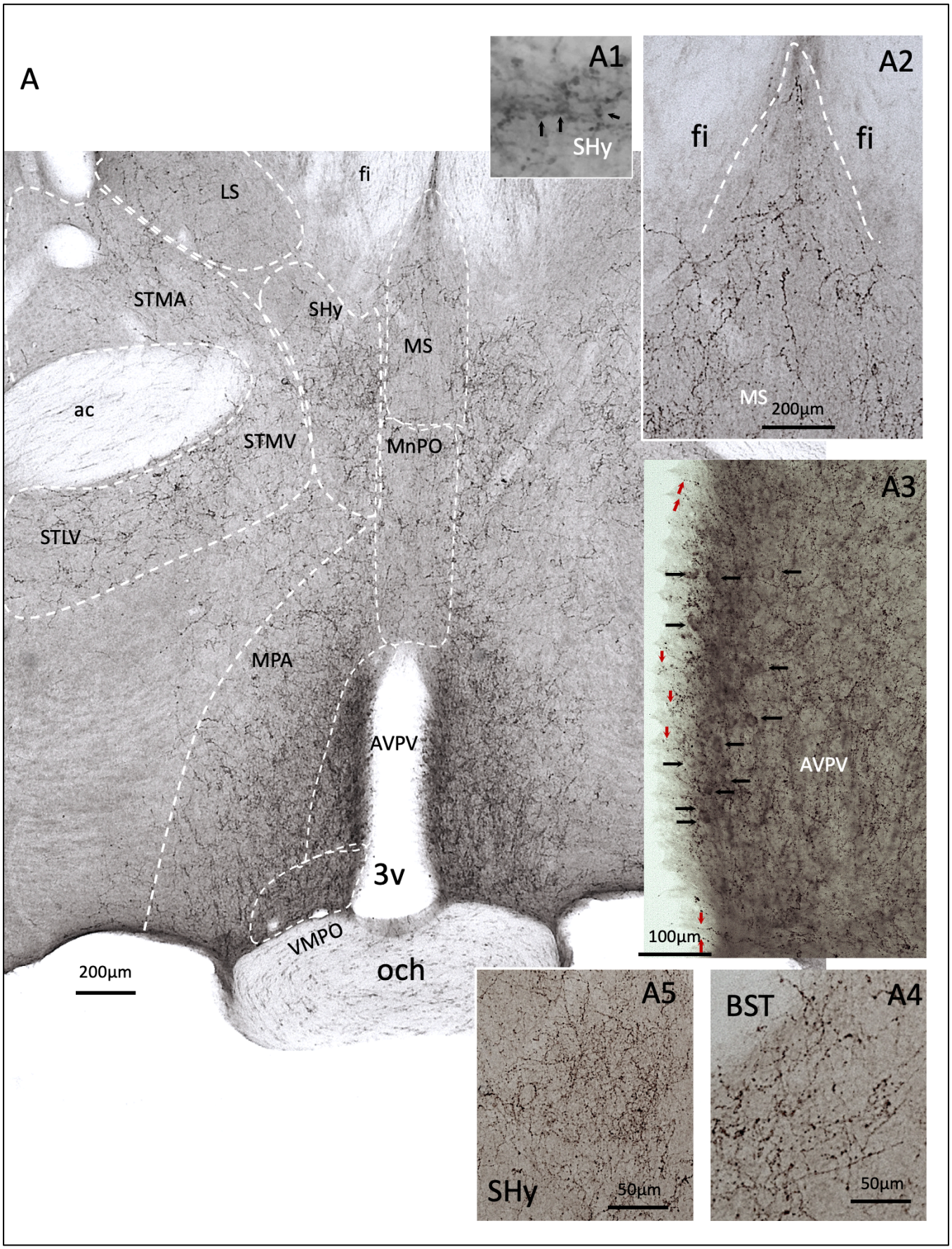
A
A1
SHy
A2
fi
fi
MS
200µm
fi
LS
STMA
SHy
MS
ac
STMV
MnPO
STLV
MPA
AVPV
3v
VMPO
och
200µm
A3
AVPV
100µm
A5
SHy
50µm
BST
A4
50µm

313

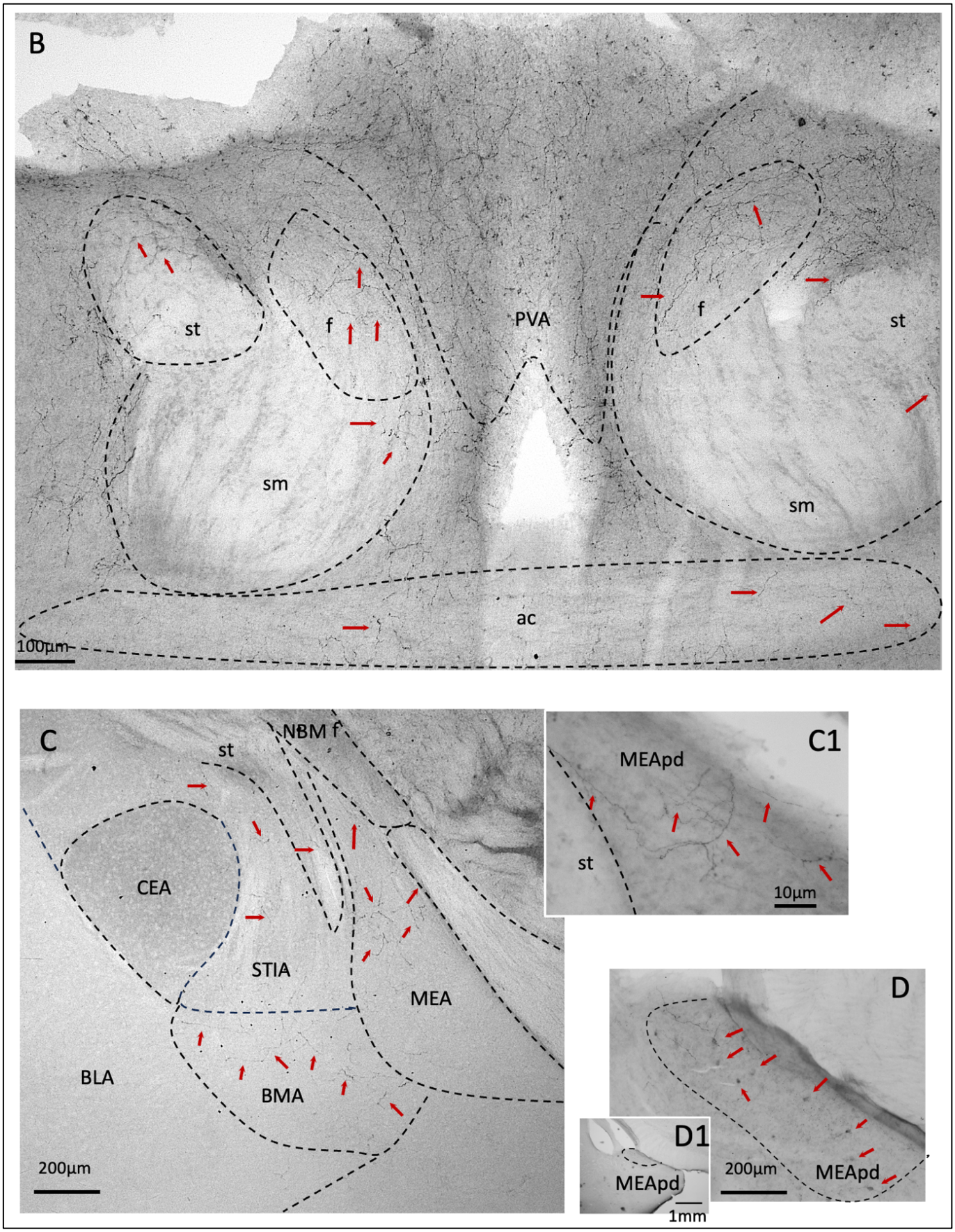
B
st
f
PVA
f
st
sm
sm
ac
100µm
C
NBM
st
CEA
STIA
MEA
BLA
BMA
200µm
C1
MEApd
st
10µm
D
D1
MEApd
1mm
200µm
MEApd

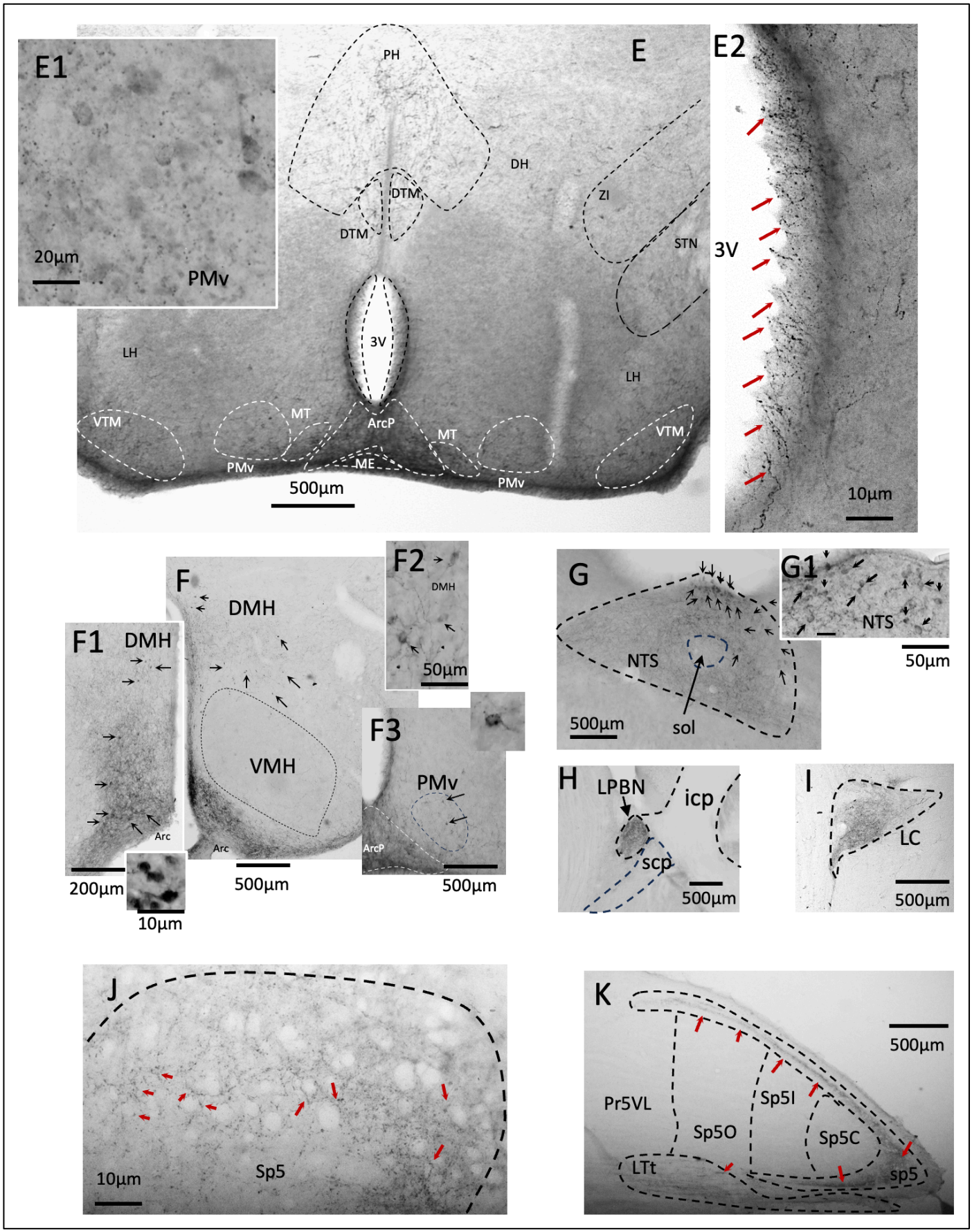
E1
20µm
PMv
E
PH
DH
DTM
DTM
ZI
STN
3V
LH
LH
VTM
MT
ArcP
MT
VTM
PMv
ME
PMv
500µm
E2
3V
10µm
F1
DMH
Arc
200µm
10µm
F
DMH
VMH
Arc
500µm
F2
DMH
50µm
F3
PMv
ArcP
500µm
G
NTS
sol
500µm
G1
NTS
50µm
H
LPBN
icp
scp
500µm
I
LC
500µm
J
Sp5
10µm
K
500µm
Pr5VL
Sp5I
Sp5O
Sp5C
LTt
sp5

Fig. 1 Mouse KP immunohistochemical reactive (-ir) distribution in controlling GnRH secretion, in comparison with other brain regions, with equally intense KP innervation, that are relevant in regulation of brain state. Panel A shows a low magnification micrograph at coronal plane (Bregma 0.38mm dorsal, 0.02mm ventral [35]), where hypothalamic kisspeptinergic regions (regions containing KP-ir cell bodies, such as the antero-ventral periventricular nucleus (AVPV,A3), ventromedial preoptic nucleus (VMPO) are shown. Besides, regions with high densities of KP innervation, which are relevant for brain state control, such as medial nucleus of preoptic area (MnPO), septo-hypothalamic nucleus (SHy, A1, A5, which also contains KP cell bodies, indicated with black arrows. For ISH image of SHy Kiss1 expressing neurons please see [1]), medial septal nucleus (MS, A2)), lateral Septal nu. (LS), bed nucleus of stria terminalis (BST, A4), with its subdivisions medio-anterior (STMA), medio-ventral (STMV) and latero-ventral (STLV). A3 shows the KP-ir in AVPV, where KP-ir neurons are indicated with black arrows and abundant KP-ir fibers innervating the ventricular surface are indicated with red arrows. Panel B, micrograph of a coronal section around Bregma -0.15mm, where 4 brain main conducting fiber systems can be clearly seen, i.e. the anterior commissure (ac), the stria medullaris (sm), the stria terminalis (st) and the fornix (f). KP-ir fibers running inside these conducting systems are indicated with red arrows. Also, the dense innervation pattern of KP-ir fibers in the paraventricular anterior nucleus of the thalamus (PVA) is shown. Panel C shown a low magnification coronal micrograph of amygdala around the coordinate Bregma -1.58mm. KP-ir fibers can be seen in stria terminalis (st), bed nucleus of stria terminalis, intra-amygdalar division (STIA), baso-medial amygdala (BMA), nu. basalis of Meynert (NBM) and medial amygdala (MEA). Interestingly, some fibers within the medial amygdala, postero-dorsal division (MEApd), are observed coming from the st, that the main axon entered the MEApd and branched locally (C1, red arrows). Panel D shows a micrograph of MEApd at Bregma -2.18mm. Numerous KP-ir cell bodies are indicated with red arrows. D1 shows a low magnification micrograph of the panel D. Panels Es and Fs show the microphotographs taken from the hypothalamic tuberal region, where the KP-ir cell bodies are seen in arcuate nucleus (Arc. E and F1), in premammillary nucleus, ventral division (PMv, E and E1, F3) and in the dorso-medial hypothalamic region (DMH, F, F1 and F2, black arrows). KP-ir fibers are observed in other regions relevant for behavioral state control at this level, such as ventral tuberomammillar nucleus (VTM), magnocelular tuberomammillar nucleus (MT) and dorsal tubero mammillary nucleus (DTM), posterior hypothalamus (PH), zona incerta (ZI) and subthalamic nu. (STN) (E). E2 shows the third ventricle at the level of Arc, posterior division (ArcP). Abundant KP-ir fibers extended toward the lumen of the ventricle (red arrows,. E2). Panel Gs- K are micrographs of samples from parasagittal sections of mouse hindbrain. Gs show the KP-ir cell bodies and dense KP-ir fibers in the solitary tract (sol) nucleus (NTS) of mouse medulla. H and I show the dense innervation pattern of KP-ir fibers in pontine nuclei: lateral parabrachial nucleus (LPBN) and locus coeruleus (LC) respectively. J and K show the dense KP-ir fibers in the spinal trigeminal tract (Sp5, K) and in the gelatinous layer of Sp5 (Ge5). Note that within the Ge5, the KP-ir fiber make perisomatic contacts with the cell bodies of the Ge5 (J, red arrows).

In Figure 2, we present chartings of mouse KP cell and fiber distribution in register with a previous study[14] for purposes of comparison. Panels A, B and C show intense KP innervation of the prefrontal structures, such as cingula cortex (Cg), dorsal peduncular cortex (DP), dorsal tenia tecta (DTT), infralimbic cortex (IL), prelimbic cortex (PrL), ventral orbital cortex (VO), nucleus accumbens shell (AcbSh), medial septal nucleus (MS), nucleus of the diagonal band of Broca (NDB) and dorsal division of the lateral septal nucleus (LSd), which were not previously reported. We also observed abundant innervation in thalamic structures such as nucleus reuniens (Re), periventricular anterior nucleus (PVA) and the epithalamic lateral habenula (LHb). In the amygdaloid complex, we observed KP innervation in cortico-amygdala (CoA), nucleus of lateral olfactory tract (NLOT), medial amygdala (MEA), mainly in the postero-dorsal division, (MEApd), basomedial amygdala (BLA), basolateral amygdala (BLA) and

nucleus of the stria terminalis, intra-amygdala division (BSTIA) (Fig. 2, D-G). Midbrain and hindbrain sensorial relay and state control centers, such as premammillary nucleus (PM), dorsal raphe nucleus (DR), periaqueductal gray (PAG), subthalamic nucleus (STh) parabrachial complex (PBc), locus coeruleus (LC), Koelliker-Fuse nucleus (KF) and nucleus of solitary tract (NTS) all possess KP-ir fibers not reported in the previous paper (Fig. 2, H-L).

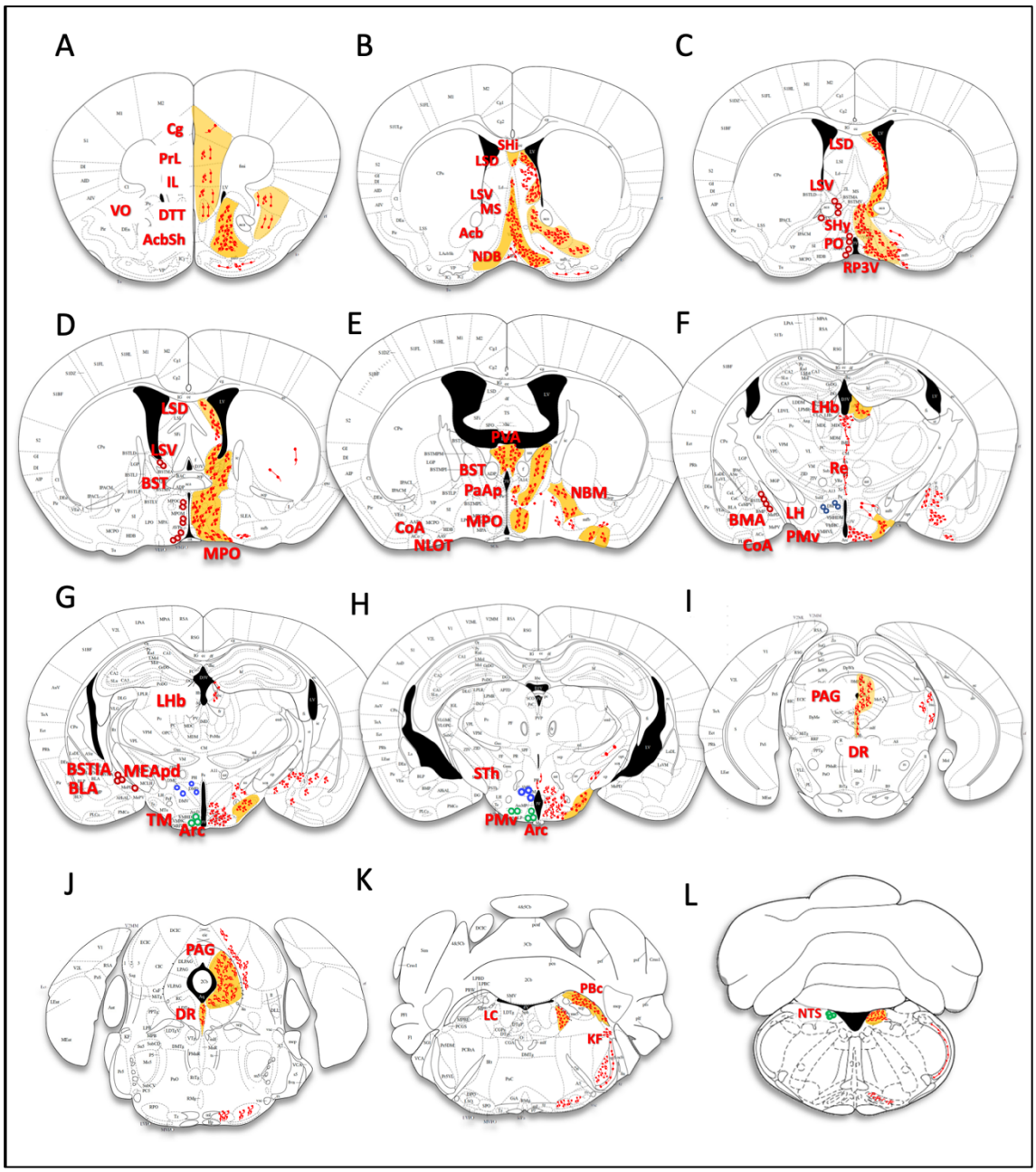

Fig. 2 Charting to represent the distribution of kisspeptin immunoreactivity in mouse brain in register with a previous study [14] for purposes of comparison. Sequential atlas planes show in the left side, KP immunoreactive cell bodies from the seven KP cell populations. Color-filled circles symbolizing the molecular signature previously reported [1]: KP-glutamatergic (green), KP-GABAergic (mainly, red) and expressing both VGLUT2 and VGAT (blue). The distribution of KP-ir fibers are represented by red lines in the right hemisphere (the thickness of the lines has been exaggerated to ensure that the lines can be seen on the atlas planes). KP-ir fibers observed in brain areas relevant for behavioral state

control are shaded in yellow: accumbens nucleus, shell (AcbSh), septohippocampal nu. (SHi), lateral septal nu. dorsal (LSD), medial septal nu. (MS), horizontal division of nucleus of dianogal band of Broca (HDB), septohypothalamic nucleus (SHy), bed nucleus of stria terminalis (BST), medial preoptic area (MPO), paraventricular anterior parvicellular division (PaAP), nucleus basalis of Meynert (NBM), lateral habenula (LHb), lateral hypothalamus (LH), tuberomammillary nu. (TM), ventral premammillary nu. (PMv), periaqueductal grey (PAG), dorsal raphe nu. (DR), locus coeruleus (LC), lateral parabrachial nu. (LPB), nu. of solitary tract (NTS). See Table 1 for remainder of abbreviations.

Kisspeptin (KP) innervation patterns in rat brain are presented in Figure 3. This figure maps KP-immunoreactive fibers (red lines) and cell bodies (blue dots) across ten septo-temporal levels of the rat brain. We observed a pattern of KP fiber distribution similar to that in the mouse brain, particularly in the hypothalamic regions. However, some qualitative differences were noted in the density and extent of KP innervation (see Table 1 for comparison between columns with titles "irGQ2 fiber rat" vs. "irGQ2 fiber mouse". A "++"-"++++" in bold indicates stronger expression in rat than mouse. The differences are especially apparent in the telencephalic and diencephalic regions, where a generally stronger KP expression was observed in rat brain. These regions include the cingulate cortex, dorsal peduncular cortex, dorsal tenia tecta, infralimbic cortex, prelimbic cortex, ventral orbital cortex, olfactory area, anterior olfactory nucleus, olfactory tubercle, extended amygdala, anterior amygdala, and accumbens shell. These differences emphasize the importance of comparative studies to understand the conserved and divergent roles of KP signaling across different species, particularly in non-reproductive functions, where KP signaling may have undergone exaptation processes allowing it to serve other relevant functions for the species in question [40].

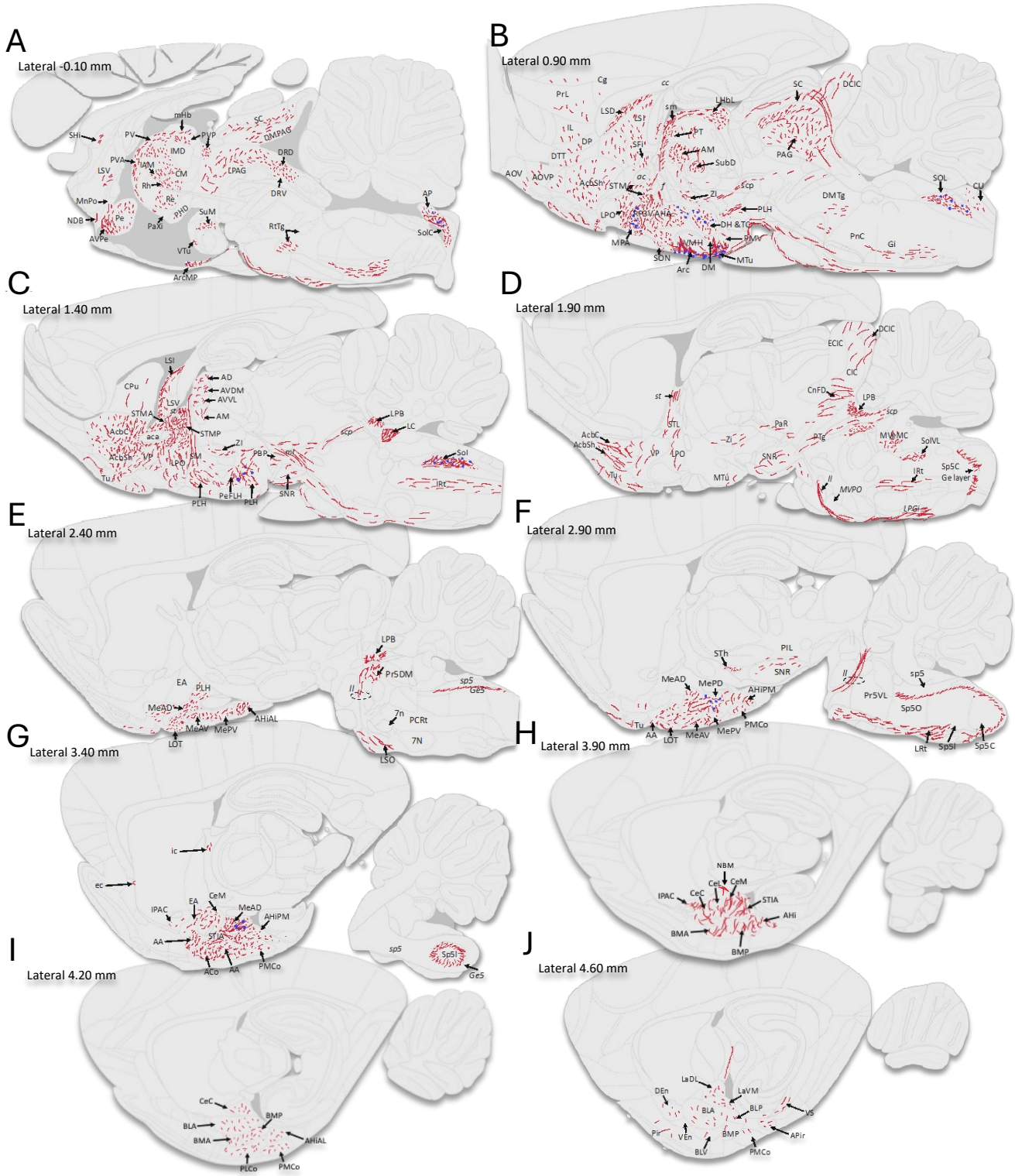

401

402 *Fig. 3 Mapping of KP immunoreactive fibers and cell bodies* ***in rat brain*** *in ten septo-temporal planes based on*
403 *microscopic observations. Blue dots represent KP-ir cell bodies and red lines represent KP-ir fibers. Relevant*
404 *anatomical regions have supporting photomicrographs form IHC-DAB reactions using the GQ2 anti-kisspeptin*
405 *antibody. See Table 1 for abbreviations.*
406 ----------

3.2 Detailed description of regional distribution of KP fibers with an emphasis on sensorial processing and behavioral state control

The distribution of kisspeptin fibers in several regions involving numerous crucial central sensorial relays and behavioral-state control structures[20-25] suggests wider participation of this peptide in other functions besides its known participation in reproduction and energy balance. In the following sections, we describe these regions in detail.

3.2.1 Telencephalon

In rodent telencephalon, the most prominent KP fiber-expressing regions are located in the *lateral septal region* in male and female mice and rats. The strongest expression was observed in the dorsal lateral septal nucleus (LSD) (Fig. 1A & A2, Fig. 2B-D, and Fig 3B-C*),* followed by ventral LS (LSV) (Fig. 2C, and 3C). LS is involved in the integration of sensorial and emotional information, and can modulate the activity of other brain regions involved in the regulation of behavioral states, such as the hypothalamus, amygdala and hippocampus[41, 42]. Recent studies have reported the main afferents of the above regions are the subdivisions of the hippocampal formation and the main efferent regions of the LSD are the ventral tegmental area and the supramammilary nucleus, whereas the LSV projects mainly to the medial hypothalamic area and medial preoptic area[42]. Activity of lateral septum can lead to changes in behavioral state, including increased exploratory behavioral, social interactions and decreased anxiety, particularly in response to social and emotional stimuli. Such behavioral changes have been reported in clinical studies with KP infusion in human subjects[43]. LS is also a key player for arousal and wakefulness, as well as for regulating processes related to mood and motivation through its extensive connections with numerous regions such as the hippocampus, amygdala, hypothalamus and with the mesocorticolimbic dopamine system[44].

The *medial septum* (MS) also contained scattered and sparse innervation in rats and mice (Fig. 1 A and 2 B). This structure is crucially involved in regulating hippocampal oscillations[45, 46], i.e. the rhythmic pattern of neuronal activity detected via changes in local field potential, which have been found to be relevant for the encoding of information and supporting processes such as learning and memory[47]. Recent studies have shown that the medial septum acts as a neural hub that regulates theta oscillations and locomotion speed, influencing goal-directed behaviors such as spatial navigation [48]. Other behaviors influenced by the medial septum include sleep, attention, learning and memory, motivation and emotional processing[49-51].

Sparse fibers were found in septofimbrial nucleus (Fig. 3B), which is an important source of cholinergic inputs to the hippocampus and the entorhinal cortex, that influence hippocampal plasticity and learning and memory under emotional stimuli; and the septohippocampal (SHi, Fig. 2B) nuclei that provide important GABAergic inputs to hippocampus playing a role in the generation of hippocampal theta oscillation[52]. The above two KPergic regions are described for the first time in this study.

Similar to Brailoiu et. al[39], we found sparse fibers in the horizontal and vertical limbs of the nucleus of diagonal band of Broca (NDB) (Fig. 2B). The diagonal band of Broca interconnects the amygdala and the septal area and projects particularly to the CA2 subfield of hippocampus, which is

involved in memory retrieval and social functions [53, 54]. It contains the second largest cholinergic neuronal population in the brain (after the nucleus basalis of Meynert)[55]. It is particularly important in the aging of the brain, since the cholinergic neuronal loss in dementias has been commonly observed in human, suggesting a possible connection between KP neuromodulation and neurodegeneration-associated cognitive dysfunction.

An interesting finding of this study was the remarkable presence of kisspeptin fibers in the *nucleus accumbens,* in both core and shell divisions (AcbC and AcbSh), with a low density in mice and a moderate density in rats (Table 1, Fig. 2A and Fig. 3B-D). AcbC receives inputs from the prefrontal cortex, the amygdala, and the ventral tegmental area (VTA), which is a key component of the brain's reward system. The AcbC integrates these inputs to evaluate the salience and value of rewards and helps to regulate motivated behavior accordingly. The nucleus accumbens shell is an important brain region involved in the processing of reward-related information and the regulation of motivated behavior, including food intake, drug seeking, and social behavior[56].

Sparse fibers were observed in the caudate putamen (CPu Fig. 2D & 3C), ventral pallidus (VP, Fig. 3D), the sustantia innominata (SI), and in main fiber pathways such as the internal capsule (ic) and external capsule (ec).

In telencephalic neocortical regions, we found sparse fibers distributed through the dorsal tenia tecta (DTT) and the dorsal peduncular (DP), prelimbic (PrL) , infralimbic (IL), and cingular (Cg) cortices, regions not reported in previous studies. The observed fibers were mainly located in layers 2/3, and no differences between species were observed (Tab. 1 and Fig. 2A & Fig. 3B). The prelimbic (PrL), infralimbic (IL) and cingulate cortices (Cg) have been classically considered to be involved in integrating the role of context in the expression of fear- or reward-induced behaviors[57-59]. The DTT and the DP have been classically involved in olfactory information processing, and recently these two structures have been shown to send inputs with information related to psychosocial stress to the dorsomedial hypothalamus, where a cardiovascular and thermogenic sympathetic stress response can be integrated[60]. In other areas classically related to the processing of olfactory information, such as the ventral and ventroposterior of the anterior olfactory nucleus, (AOV and AOVP) and the olfactory tubercle (Tu), we found sparse fibers only in the rat (Tab. 1, Fig. 3B-D).

In the amygdalar complex, we confirmed the KP-ir cell population mainly confined within the medial amygdala's postero-dorsal division (MePD) which has been reported already elsewhere [61, 62] (Table 1 & Figs. 1C-D, 2F-G and 3F-G). ISH study in gonadally intact rats and mice showed that *Kiss1* levels were higher in males than females and fluctuated with the estrous cycle, peaking at proestrus in rats [63] suggesting its potential influence reproductive and broader brain functions. Kisspeptin-immunolabelled neurons in the MePD and an axon terminal process were observed to innervate the adjacent nucleus of the stria terminalis intra-amygdaloid division and the stria terminalis. Also, we observed KP-expressing cell bodies in the septo-hippocampal (SHi) and septo-fimbrial (SFi) region surrounding the anterior commissure, and extending into the septum. These neurons were characterized neurochemically in mice in our previous report[1].

494 In relation to density of fibers in the septo-bed nucleus of stria terminalis complex, regions with a
495 moderate/intense density of fibers were found within the septal part of the bed nucleus of the stria
496 terminalis (BSTMA, BSTMP, BSTLV and BSTLP, Fig. 1A; Fig. 2B-D and Fig. 3B-C). The temporal
497 intra-amygdala division of the BST (BSTIA, Fig. 1C; Fig. 2F and Fig. 3H) showed a selective expression
498 of KP fibers. Other regions in the extended amygdala that also showed low/scattered expression of KP
499 fibers were the central amygdalar nucleus (CeC and CeM Fig. 3G-H) and the medial amygdalar nucleus
500 (MePD and MePV Fig. 2,F-G and Fig. 3.G-H). Sparse fibers were found in the oval nucleus of the stria
501 terminalis (BSTLD), the basolateral amygdala (BLA), the basomedial amygdala (BMA), the lateral part
502 of the central amygdalar nucleus (CeL), the cortico-amygdala (CoA) the nucleus of the lateral olfactory
503 tract (NLOT) and the stria terminalis (st, Fig. 1C). Compared with the study of Brailou et al, here we
504 report the presence of fibers in the anterior, medial, and cortical amygdala and the intra-amygdaloid
505 division of the stria terminalis (Tab. 2).
506
507 *3.2.2. Diencephalon*
508
509 The *hypothalamus* contains four of the seven KP neuronal populations described in detail here and in a
510 companion report[(1)], i.e. the rostral periventricular (RP3V) population mainly located in the medial
511 preoptic area (MPO) and in the anteroventral periventricular area (AVPe); the arcuate (Arc) population;
512 the dorsomedial hypothalamus (DMH); and the ventral premammillary nu. (PMv) (Fig. 1A; Fig. 2 C, D,
513 F, G, H and Fig. 3B). After a careful analysis of immunoreacted serial sections, and following the
514 pathways of the labelled fibers, we identified some extrahypothalamic regions likely to be targets of these
515 regions. Ascending fibers originating in the RP3V population travel lateral-dorsal-caudally toward the
516 stria medularis (sm), and the stria terminalis (st) conduction systems (Fig. 1, B). In their path, they
517 extensively innervate the bed nucleus of the stria terminalis (Tab. 2). It is worth noting the presence of KP
518 fibers innervating the border between the *medial (MHb) and lateral (LHb) habenula* (Fig. 2, F-G and Fig.
519 3 B), as it is known that the main input to the habenula is the stria medullaris (*sm*). Other fibers originating
520 in the MPO/AVPV region travel to innervate the organum vasculosum of the lamina terminalis (OVLT)
521 and then ascend dorsally and laterally to innervate the *accumbens core* (AcbC) and the *lateral septum*
522 regions.
523
524 We observed high-moderate densities of KP-ir fibers (see Tab. 2) in the caudal periventricular area
525 and ventral periventricular areas of the arcuate nucleus (Arc, Fig. 1E, and Fig. 2F-H). Some targets of the
526 KP neural population in the posterior hypothalamus were identified by following the labelled axon in
527 serially collected sections in coronal and parasagittal planes Some fibers originating in the Arc travelled
528 in the base of the brain reaching the internal capsule (ic) and optic tract through which they travel in a
529 path to the subthalamic nucleus (STh), the lateral part of the supramammillary nucleus (SuML) and
530 continuing to the central nucleus of the amygdala (CeA). Some efferent fibers traveled caudally to
531 innervate the ventral premammillary nucleus (VPM), the ventral tuberomammillary nucleus (VTu), and
532 the supramammillary nucleus (SuM). Additional fibers surrounded the ventromedial hypothalamus (VMH)
533 and travelled dorsally to innervate the anterior hypothalamic area, continuing on to innervate medial nuclei
534 of the thalamus including the paraventricular thalamic (PVT). The latter showed the highest innervation,
535 albeit the intermediodorsal (IMD) the centromedial (CM), mediodorsal (MD), paratenial (PT), rheuniens
536 (Re) and rhomboid (Rh) nuclei of the thalamus also contained KP-ir fibers.
537

538 The population of weakly KP-immunopositive cells scattered in the medio-lateral dorsal
539 hypothalamic area (DH) spanning from the posterior part of the anterior hypothalamus (AHp) to the
540 posterior hypothalamus (PH), and centered in the tuber cinereum area (TC) (Fig. 1F; Fig. 2F-H, and Fig.
541 3B) were observed to project to adjacent zona incerta (ZI). Finally, the last population of KP neurons in
542 the PMv was very weakly labelled and it was not possible to identify the axonal projections.
543
544 Other regions in the hypothalamus containing KP fibers are the median preoptic nucleus (MPO),
545 the parastriatal nucleus (PS), the paraventricular nucleus medial magnocellular division (PVNmm) and
546 the parvocellular division (PVNmp), and in rat also the ventral premammillary nucleus (PMv), ventral
547 tuberomammillary nucleus (VTu), and suprammamilary nucleus (SuM). A low density of fibers was
548 observed in dorsomedial hypothalamic nucleus, MPO, lateral preoptic area, periventricular hypothalamic
549 nucleus anterior (PVa), and supraoptic nucleus (SO). Sparse fibers were found in the dorsal hypothalamus
550 (DH), zona incerta (ZI), lateral hypothalamic area (LH), posterior hypothalamic area (PH), retrochiasmatic
551 area (RCh), and ventromedial hypothalamic nucleus (VMH). These observations confirm and extend
552 extensive investigations of the hypothalamic KP system[16].
553
554 In the thalamus, the highest density of fibers was observed in the paraventricular thalamic nucleus
555 (PVT) in rats and mice (Fig. 1B; Fig. 2E-F and 3B). Low fibers densities were also observed in other
556 nuclei of the thalamus, such as in the centromedial (CM), mediodorsal (MD), paratenial (PT), reuniens
557 (Re), and rhomboid (Rh). The epithalamic habenular nucleus (Hb) showed a moderate density of fibers
558 mainly located in the border between its medial and lateral subdivisions (Fig. 2F-G and 3B), with some
559 of these fibers arriving through the stria medullaris.
560
561 *3.2.3. Mesencephalon*
562
563 Within the mesencephalon, Brailoiu et al[39] reported a sparse number of kisspeptin-immunoreactive fibers
564 only in the dorsomedial periaqueductal gray substance (DMPAG). In our study this region had the highest
565 density of kisspeptin fibers within the mesencephalon (Fig. 2J and Fig. 3B). However, we also visualized
566 scattered fibers in the central nucleus of the inferior colliculus (CIC, Fig. 2I and Fig. 3D), dorsal raphe
567 nucleus (DR, Fig. 2J and Fig. 3A), and sparse fibers in the deep mesencephalic nucleus (DpMe),
568 interpeduncular nucleus (IP), median raphe nucleus (MnR), substantia nigra (SN), intermediate and deep
569 gray layer of the superior colliculus (DpG), supramammillary nucleus (Sum), substantia nigra pars
570 reticulata (SNpr) and ventral tegmental area (VTA). The functional implications for those Kp projections
571 are not yet ascertained.
572
573 *3.2.4. Metencephalon and myelencephalon*
574
575 In the metencephalon and myelencephalon, we observed kisspeptin immunopositive cell bodies in the
576 *nucleus tractus solitarius* (NTS or Sol), and *area postrema* (AP) Fig. 1 G; Fig. 2L and Fig. 3A-D). We
577 did not observe immunopositive neurons in the caudoventrolateral or the lateral reticular nuclei (CVL and
578 LRt), nor the spinal trigeminal tract, as reported in Brailoiu et al[39]. With respect to the density of the
579 fibers, intense labelling was found in the lateral parabrachial nucleus (LPB, Fig. 1H, Fig. 2K), the Kolliker-
580 Fuse nucleus (KF Fig. 2K), NTS, (Fig. 1G; Fig. 2L and Fig. 3A-D) in the dorsomedial part of the principal

581 sensorial component of the trigeminal nucleus (Pr5DM, Fig. 1K and Fig. 3D-G) and locus coeruleus (LC,
582 Fig. 1I; Fig. 2K and Fig. 3C). The rat brain also showed intense Kp labeling in the gelatinous layer and
583 the spinal nerve 5 (Fig. 1J-K and Fig. 3E-F). Moderate density was observed in the superior cerebral
584 peduncle (scp) . Low intensity was observed in several nuclei of the reticular formation, including the
585 caudoventral reticular nucleus (CVL), the gigantocellular reticular nucleus (Gi), the intermediate reticular
586 nucleus, the lateral reticular nucleus (LRt), the medullary dorsal reticular nucleus (MdD), the parvicellular
587 reticular nucleus (PCRt), and the rostroventrolateral reticular nucleus (RVL). Sparse fiber density was
588 observed in the ambiguus nucleus (Amb); lateral superior olive (LSO); ventral medullary reticular nucleus
589 (MdV); in subregions of the pontine nucleus such as the brachium pontis (bpPn), the reticular oral part
590 (PnO), and the reticular caudal part (PnC); and in the raphe magnus (RMg), obscurus (Rob), and pallidus
591 (RPa).
592
593 3.3 KP fiber density: sex differences and short- and long-term effects of gonadectomy
594
595
596 Numerous studies have reported that gonadal status affects *Kiss1* expression, with KP^{Arc} expression
597 decreased, and rostral hypothalamus KP^{RP3V} expression increased by gonadal steroids[64-66]. We have also
598 reported male and female *Kiss1* expression differences and acute sensitivity to GNX (i.e. within 4-7 weeks
599 of GNX)[1].
600
601 We extensively studied the fiber distribution in male and female mice that underwent gonadectomy
602 in young adulthood (3 month old). The experimental subjects were perfused/fixed at ages of 4-5 months
603 (1-2 months after GNX) or 15 months (12 months after GNX). We examined KP-ir fibers densities aiming
604 to assess if there are sex differences in KP fiber distribution and whether castration modifies the density
605 of fibers apparent both shortly after GNX, and in aged mice after early GNX, compared with intact
606 subjects of the same age.
607
608 Supplementary Information Figure 1 shows the cumulative (summed) fiber density charting of
609 three young adult animals from each of four groups: male/female intact and male/female gonadectomized.
610 The chartings were made under microscopical observation and verified by two junior and two senior
611 experimenters of this research team. The cumulative fiber densities displayed in the SI Figure 1 show no
612 appreciable differences among the four groups following careful analysis of KP-ir fiber density across
613 groups. This may be due to a lack of regulation of KP production in any of the neuronal groups
614 contributing nerve terminals to the assessed areas, or, possibly, compensatory and opposite regulation of
615 KP production among multiple contributing KPergic inputs to a given region.
616
617 We further made an analysis of KP Cre-driver in ARC and RP3V tracing experiments performed
618 by the Allen Brain Institute and deposited in the Allen Brain Atlas (showed in the last two columns of the
619 table 1). In the supplementary information (SI) figure 1, we highlight the projection targets of R3PV or
620 Arc *Kiss1*-Cre neurons transfected with AAV. The data from two *Kiss1*-Cre mice injected in the arcuate
621 nucleus (Arc, experiments 232311236 and 232310521) and two *Kiss1*-Cre mice injected in the rostral
622 periventricular region (R3PV, experiments 299247009 and 301989585) are reproduced in this Figure. The
623 VGAT-expressing *Kiss1* R3PV neuronal population and its projections are represented in red, and the
624 VGLUT2-expressing *Kiss1* Arc population and its projections are represented in green. The different

625 views show a reciprocal dense innervation between the Arc and the RP3V. Additionally it is clear that the
626 majority of regions in the striatum, septum, BNST, thalamus, hypothalamus, and amygdala receive
627 convergent innervation from both Arc and RP3V Kiss1 neuronal populations.
628
629 According to our KP fiber study, and analysis of the Allen Connectivity Map, a representation of
630 the relative fiber density distribution and some identified kisspeptin pathways through the mouse brain is
631 presented in the flat map in SI Figure 3. Most of the regions involved in sensorial processing, motor
632 integration and behavioral state control that were described and discussed previously are shown in this
633 representation with reciprocal or convergent innervations from both KP-RP3P and KP-Arc.
634
635 Table 2 is a report of a semiquantitative analysis of 22 regions from 12 15-month old mice, within
636 the scope of this study. In female subjects, 19 of the 22 regions were found similar in term of density of
637 KP-ir fibers between old intact ("FC" stands for female control) and experimental ("OVX" stands for
638 ovariectomy performed 12 months prior to perfusion/fixation) female mice. The septohypothalamic
639 nucleus showed increased KP-ir fiber density in OVX subjects. This region, beside hosting
640 *Kiss1/Slc32a1/Ar* expressing neurons[(1)] (Fig. 1, A and A1), receives direct $RP3V^{KP}$ and Arc^{KP} projections
641 as shown by Allen Mouse Brain Atlas (SI figure 1). Hence, the source of the neuronal cell group
642 contributing to the increased KP-ir fiber density in septohypothalamic nucleus after OVX is not clear. In
643 the RP3V and MPO region, the samples from OVX subjects also showed an increased KP
644 immunoreactivity (Fig. 4). This region, besides hosting a KP neuronal population itself, also receives
645 Arc^{KP} axonal projections, as demonstrated in SI Figure 1. In male subjects, 18 of the 22 regions showed
646 no apparent differences between intact ("MC" stands for male control) and orchiectomized ("ORX" stands
647 for orchiectomy) male mice. Three regions exhibited higher densities of KP-ir fibers in the ORX group
648 compared to the aged-matched intact controls: dorsal hypothalamus (DH, Fig. 4), paraventricular anterior
649 thalamus (PVA) and tuberomammillary nucleus (TM). Also, in these three regions, the MC group showed
650 higher densities than the FC group (Fig. 4).
651
652 Table 2 Semiquantitative analysis of KP immunopositive cells and fiber density in regions hosting
653 KPergic neurons and regions related to sensorial-brain state processing in old female and male mice
654

	FC	OVX	FC vs OVX	MC	ORX	MC vs ORX	FC vs MC
AcbSh	+++	+++	FC ≈ OVX	++	++	MC ≈ ORX	FC > MC
Arc	+++	+++	FC ≈ OVX	++	++	MC ≈ ORX	FC > MC
BSTam	+++	+++	FC ≈ OVX	++	++	MC ≈ ORX	FC > MC
DB	+++	+++	FC ≈ OVX	+	++	MC ≈ ORX	FC > MC
DH	+	+	FC ≈ OVX	++	++	MC < ORX	**FC < MC**
LC	++++	++++	FC ≈ OVX	++++	++++	MC ≈ ORX	FC ≈ MC
LSD	+	+	FC ≈ OVX	+	+	MC ≈ ORX	FC ≈MC
MEA	+	+	FC ≈ OVX	+	+	MC ≈ ORX	FC ≈ MC
MS	++	++	FC ≈ OVX	+	+	MC ≈ ORX	FC > MC
NTS	++++	++++	FC ≈ OVX	++++	++++	MC ≈ ORX	FC ≈ MC
PaAP	+++	+++	FC ≈ OVX	++	++	MC ≈ ORX	FC > MC
PBN	++++	++++	FC ≈ OVX	++++	++++	MC ≈ ORX	FC ≈ MC
TM	+	+	FC ≈ OVX	++	++	MC < ORX	**FC < MC**

PMv	+	+	FC ≈ OVX	++	++	MC ≈ ORX	**FC < MC**
PVA	++	++	FC ≈ OVX	+++	++++	MC < ORX	**FC < MC**
PVN	+++	+++	FC ≈ OVX	++	++	MC ≈ ORX	FC > MC
RP3V	+++	++++	FC < OVX	++	++	MC ≈ ORX	FC > MC
AH (adj SCN)	+++	+++	FC ≈ OVX	++	++	MC ≈ ORX	FC > MC
SHy	+++	++++	FC < OVX	++	++	MC ≈ ORX	FC > MC
STIA	+	+	FC ≈ OVX	+	+	MC ≈ ORX	FC ≈ MC
Wall 3V	+++	+++	FC ≈ OVX	+	+	MC ≈ ORX	FC ≈ MC
ROIs adj. (f/st/sm/ac)	++	++	FC ≈ OVX	++	++	MC ≈ ORX	FC > MC

Table 2. Semiquantitative comparison of kisspeptin immunoreactive cell and fiber distribution in KP expressing regions of control vs gonadectomized mice. Since no differences in the direction of changes were observed in male vs female mice the data reflected here is derived from pooled observations from both sexes. n.a.: not applicable. FC: female control (intact 15 mo. old); OVX: 12 mo. post-ovariectomy (15 mo. old); MC: male control (intact 15 mo. old); ORX: 12 mo. post-orchiectomy (15 mo. old); AcbSh, nucleus accumbens shell; Arc, arcuate nucleus; BSTam, bed nucleus of stria terminalis, anteromedial division; DB, nucleus diagonal band de Broca; DH, dorsal hypothalamus; LC, locus coeruleus; LSD, lateral septal nucleus, dorsal division; MEA, medial amygdala; MS, medial septal nucleus; NTS, nucleus of tract solitary; PaAP, paraventricular nucleus anterior parvocellular division of the hypothalamus; PBN, parabrachial nucleus and pons; TM, tuberomammillary nucleus of the hypothalamus; PMv, Premammillary nucleus, ventral subdivision of the hypothalamus; PVA, paraventricular nucleus anterior division of the thalamus; PVN, paraventricular nucleus of the hypothalamus; RP3V, rostro-periventricular complex of third ventricle of the hypothalamus; AH anterior hypothalamic area (adjacent to suprachiasmatic nucleus, SCN); SHy, septo-hypothalamic nucleus; STIA, nucleus of stria terminalis, intra-amygdalar division; Wall 3V, ependymal layer of the 3rd ventricle; ROIs adj. (f/st/sm/ac), regions of interest adjacent to brain conducting system (fornix, f, stria terminalis, st, stria medullaris, sm, anterior commissure, ac).

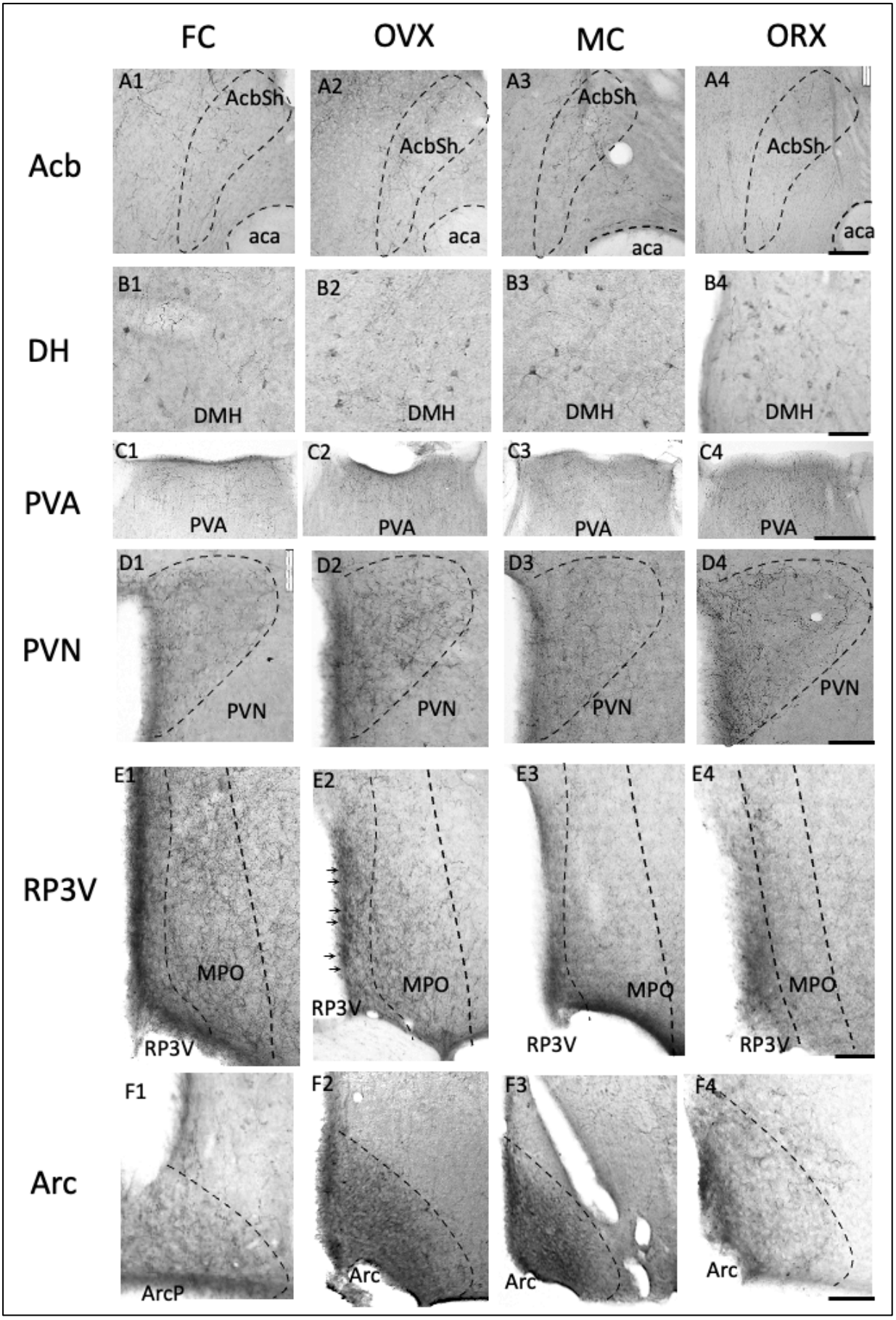
FC
OVX
MC
ORX
Acb
DH
PVA
PVN
RP3V
Arc
A1
AcbSh
aca
A2
AcbSh
aca
A3
AcbSh
aca
A4
AcbSh
aca
B1
DMH
B2
DMH
B3
DMH
B4
DMH
C1
PVA
C2
PVA
C3
PVA
C4
PVA
D1
PVN
D2
PVN
D3
PVN
D4
PVN
E1
MPO
RP3V
E2
MPO
RP3V
E3
MPO
RP3V
E4
MPO
RP3V
F1
ArcP
F2
Arc
F3
Arc
F4
Arc

674

675
676 *Fig. 4 Examples of KP-ir fiber density in old mice: comparison of four groups. FC: samples from female*
677 *control, intact mice of 15-month-old; OVX: female mice undergoing ovariectomy in young adulthood (3-*
678 *month-old) and perfused/fixed 12 months after OVX); MC: male intact mice; ORX: male mice undergoing*
679 *orchiectomy in young adulthood (3 month old) and perfused/fixed 12 months after ORX). Acb, nucleus*
680 *accumbens; AcbSh, nucleus accumbens shell: Arc, arcuate hypothalamic n.; ArcP, arcuate hypothalamic*
681 *n. posterior; DH, dorsal hypothalamus; DMH, dorsomedial hypothalamus; PVA, paraventricular nucleus*
682 *anterior division of the thalamus; PVN, paraventricular nucleus of the hypothalamus; RP3V, rostro-*
683 *periventricular complex of third ventricle of the hypothalamus. Scale bars: 100µm.*
684 ----------
685
686 3.4 Mapping of *Kiss1r and its co-expression with Slc32a1, Slc17a6 and Kiss1* with RNAscope methods:
687 assessment of *Kiss1r* distribution in CNS and assessment of Kiss1-Kiss1r co-expression
688
689 Using RNAscope dual and multiplex ISH methods, we report here (Fig. 5) semi-quantitative expression
690 levels of *Kiss1r*, depicted as different intensities of blue shading, in mouse brain sagittal serial sections. In
691 contrast to the discrete expression of *Kiss1* in seven neuronal populations in brain[(1)], *Kiss1r* expression is
692 diffuse and widespread. *Kiss1r* was preferentially expressed in non-GABAergic neurons (Table 3), such
693 as hippocampal projection neurons, mainly glutamatergic thalamic nuclei, mammillary complex neurons,
694 cerebellar granule cells, and the interposed nucleus. *Kiss1r* was also co-expressed with *Kiss1* itself in
695 hypothalamic neurons, suggesting an autocrine component of KP signaling in the hypothalamus. For
696 example (Fig. 6, panel 14 and 17) *Kiss1r* and *Kiss1* are co-expressed in RP3V, using 4-channel RNAscope
697 LS Multiplex Fluorescent Assay against mRNA for kisspeptin receptor (*Kiss1r*, red dots), kisspeptin
698 (*Kiss1*, green dots, VGAT (*Slc32a1*, blue dots) and VGLUT2 (*Slc17a6*). In RP3V (Fig. 6, panel 14), six
699 out of nine cells (6/9) in a representative confocal microphotograph of this area co-expressed the four
700 mRNAs (indicated with quadri-color-arrows). This is in accordance with our previous observation [(1)] that
701 the kisspeptinergic neuronal population in the RP3V co-express VGAT and VGLUT2 mRNA, indicating
702 the GABA/Glutamate co-transmission nature of those subcortical neurons. Three cells not expressing
703 Kiss1+ but expressing Kiss1r were Slc32a1^{-} and Slc17a6^{+}. In Arc (Fig. 6, panel 16), Kiss1r was also found
704 co-expressed in Kiss1- and Slc17a6-expressing cells lacking expression of Slc32a1 (indicated with tricolor
705 arrows in the panel 16). Insets show 4-channel separated screenshots of the cell in the center. The red thin
706 arrows, generated by the Leica Application Suite (LAS) software, indicate the very same coordinates in
707 each channel. While previous studies[(31, 67)] have reported exclusive expression of Kiss1 and Kiss1r in
708 hypothalamus, careful inspection of the reported data suggest that co-expressing cells may be
709 undercounted without optimal *colocalization at the cellular level* and employment of precise and enhanced
710 image processing tools. Panel 12 of Fig. 6, depicts expression of Kiss1r in each of the cells in the ventral
711 division of the premammillary nucleus (PMv), a region recently reported to host the newly discovered
712 KP population. Most neurons neighboring *Kiss1-expressing* cells also expressed *Kiss1r*, suggesting that
713 the KP/Kiss1R pathway may use *paracrine* mechanisms, as well as autocrine ones, in addition to classical
714 neurotransmission through axon innervation and transmitter co-release, and potentially Kp humoral
715 function via release into cerebrospinal fluid (Fig. 1, Panels A3 and E2).

716

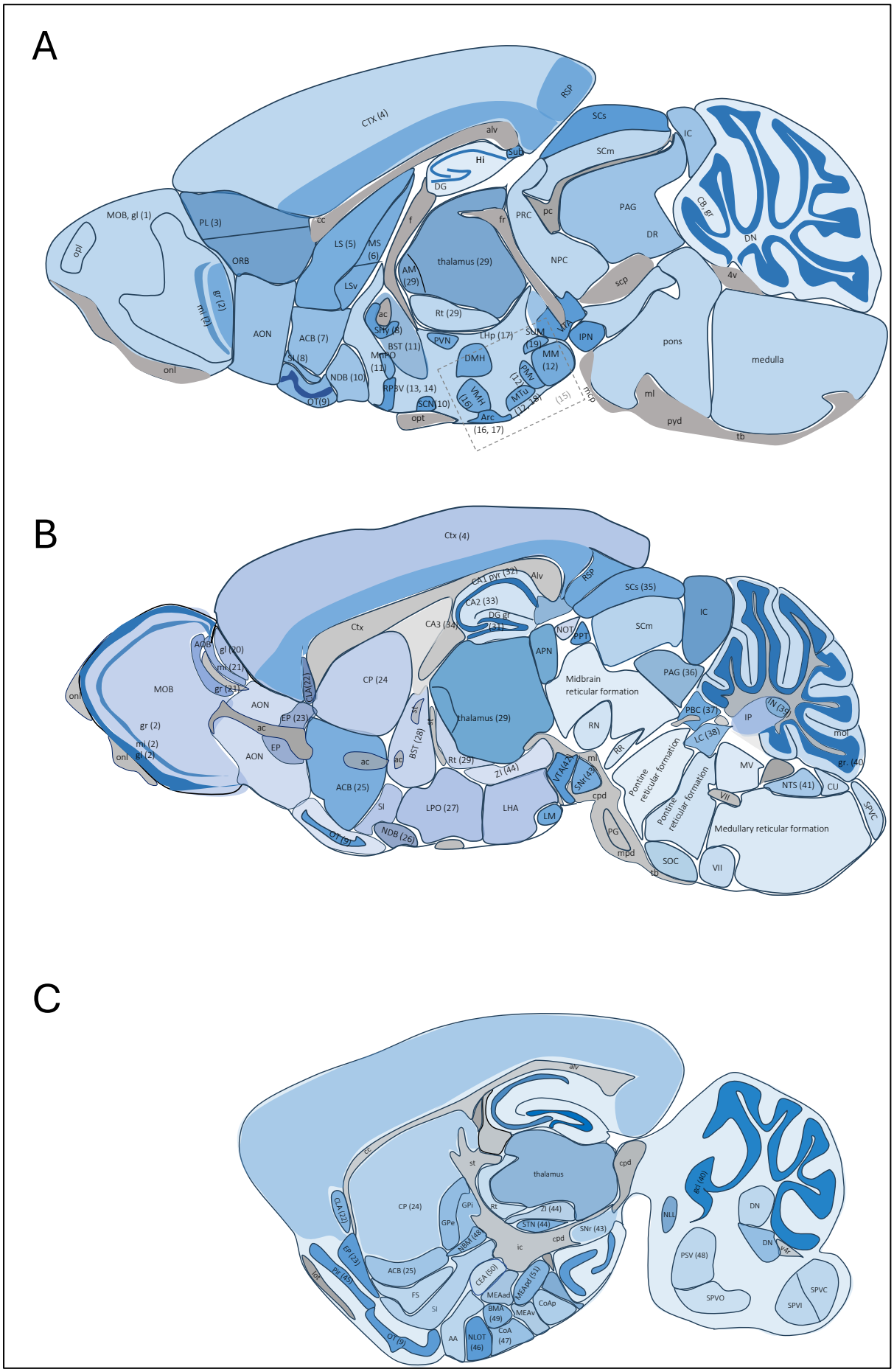
A
CTX (4)
RSP
alv
Sub
Hi
DG
SCs
SCm
IC
PAG
DR
CB, gr
DN
4v
PRC
pc
fr
NPC
scp
MOB, gl (1)
PL (3)
opl
ORB
cc
LS (5)
MS (6)
f
thalamus (29)
AM (29)
LSv
gr (2)
mi (2)
AON
ac
SHy (8)
Rt (29)
ACB (7)
BST (11)
PVN
LHp (17)
SUM (19)
VTA
IPN
pons
medulla
SI (8)
MnPO (11)
DMH
MM (12)
NDB (10)
RPBV (13, 14)
PMv (12)
VMH (16)
MTu (12, 18)
(15)
mcp
ml
OT (9)
SCN (10)
opt
Arc (16, 17)
pyd
tb
onl
B
Ctx (4)
CA1 pyr (32)
Alv
RSP
SCs (35)
CA2 (33)
DG gr (31)
IC
Ctx
CA3 (34)
NOT
PPT
SCm
AOB
gl (20)
mi (21)
APN
CP (24)
Midbrain reticular formation
PAG (36)
MOB
gr (21)
CLA (22)
AON
thalamus (29)
PBC (37)
IN (39)
IP
gr (2)
EP (23)
st
RN
LC (38)
mol
mi (2)
ac
EP
BST (28)
RR
gl (2)
AON
ac
ac
Rt (29)
ml
Pontine reticular formation
MV
gr. (40)
ACB (25)
Zl (44)
VTA (42)
SNr (43)
cpd
NTS (41)
CU
SI
LPO (27)
LHA
VII
SPVC
LM
Pontine reticular formation
Medullary reticular formation
OT (9)
NDB (26)
PG
mpd
SOC
VII
tb
C
alv
cc
st
thalamus
cpd
CP (24)
GPi
Rt
Zl (44)
Bcl (40)
NLL
DN
CLA (22)
GPe
STN (44)
SNr (43)
NBM (48)
cpd
ic
DN
v4r
EP (23)
PSV (48)
ACB (25)
CEA (50)
MEAad
MEAad (51)
Pir (45)
lot
FS
SI
BMA (49)
MEAv
CoAp
SPVO
SPVC
SPVI
OT (9)
AA
NLOT (46)
CoA (47)

717 ***Fig. 5 Mapping of Kiss1r (RNA encoding KP receptor) expression*** (symbolized by the intensity of blue shading)
718 in three septo-temporal planes (A-C) based on microscopical observation reported in the table 2. Numbers following
719 region-abbreviations correspond to the panel numbers of Figure 6. ACB, nucleus accumbens; AM, anteromedial
720 nucleus of thalamus; AOB gr, granule cell layer AOB; AOB ipl, inner plexiform layer AOB; AOB mi,
721 mitral cell layer AOB; AOB opl, outer plexiform layer AOB; AOB, glomerular layer AOB; MOB, main
722 olfactory bulb; Arc, arcuate hypothalamic n.; BMA, basomedial amygdala; BST, bed nucleus of stria
723 terminalis; CEA, central amygdala; CLA, Claustrum; CoA, corticoamygdala; CP, caudoputamen; DC,
724 dentate gyrus; EP, endopiriform n.; gcl, granule cell layer of DG; gr, cerebellar granule cell layer; LC,
725 locus coeruleus; LPO, lateral preoptic area; LS, lateral septal n. ; MEA, medial amygdala; MnPO, median
726 preoptic n.; MOB, main olfactory bulb; MOB gl, glomerular layer MOB; MOB gr, granule cell layer MOB;
727 MOB ipl, inner plexiform layer MOB; MOB mi, mitral cell layer MOB; MOB opl, outer plexiform layer
728 MOB; Mol, cerebellar molecular cell layer; MS, medial septal n.; NBM, nucleus basalis of Meynert; NDB,
729 diagonal band nucleus; NLOT, nucleus of lateral olfactory tract; NTS, nucleus tractus solitarii; OT,
730 olfactory tubercle; PAG, periaqueductal grey; PB, parabrachial n.; PC, Purkinje cell; PfC, prefrontal
731 cortex; Pir, piriform cortex; PL, prelimbic area; plc, pyramidal cell layer; PMv, premammillary n., ventral;
732 RP3V, rostro-periventricular n. of 3rd ventricle; Rt, reticular thalamic nucleus; SC, superior colliculus;
733 SCN, suprachiasmatic n.; scp, superior cerebellar peduncle; SHy, septo-hypothalamic n.; SNr, substantia
734 nigra reticulata; SS, somatosensorial cortex; STN, subthalamic nucleus; SUM, supramammillary n.; TMv,
735 tuberomammillary n., ventral; VMN, ventromedial hypothalamic n.; VTA, ventral tegmental area; ZI,
736 zona incerta.
737 ----------
738

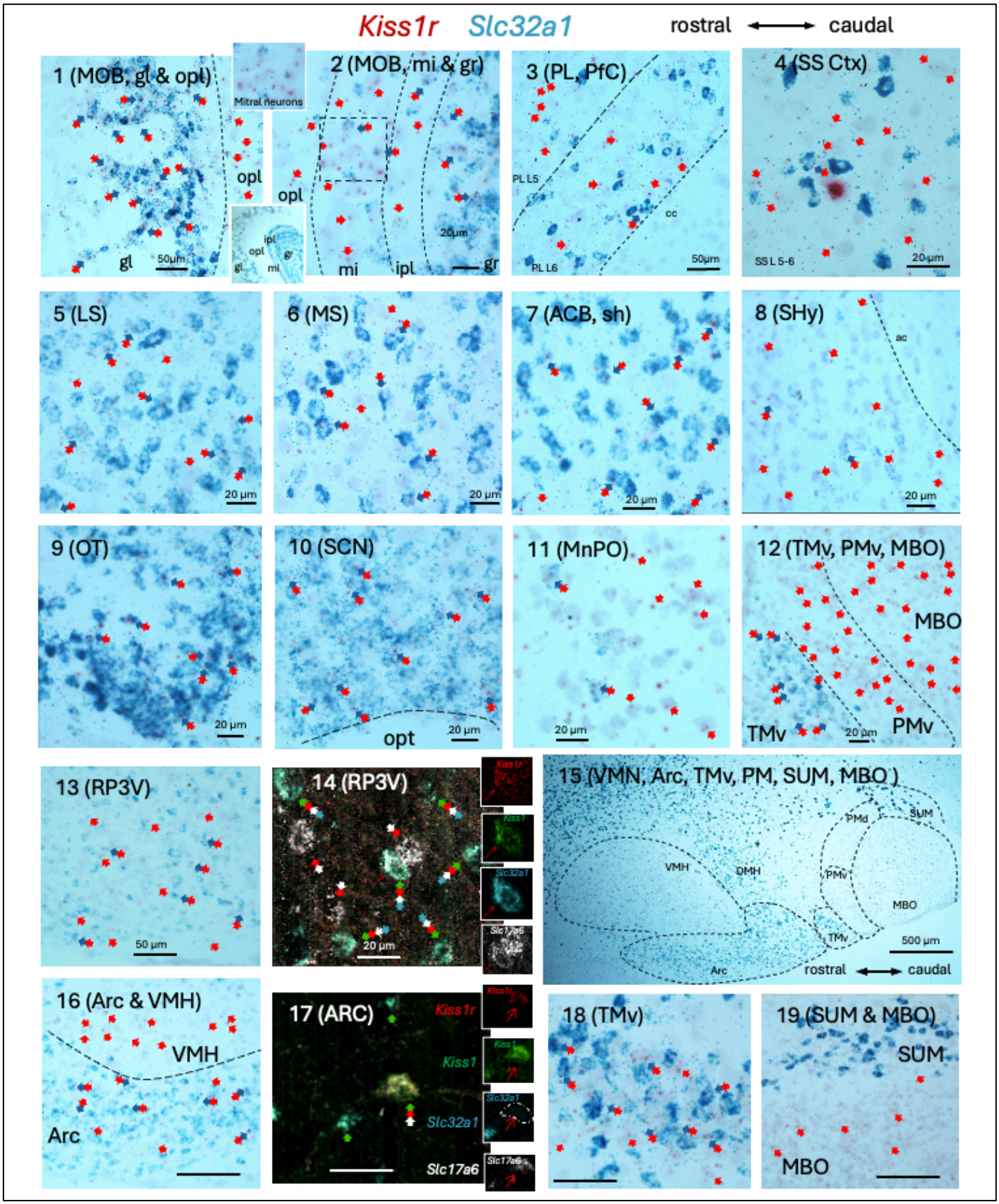
Kiss1r
Slc32a1
rostral
caudal
1 (MOB, gl & opl)
Mitral neurons
opl
gl
50µm
2 (MOB, mi & gr)
opl
mi
ipl
gr
20µm
3 (PL, PfC)
PL L5
cc
PL L6
50µm
4 (SS Ctx)
SS L 5-6
20 µm
5 (LS)
20 µm
6 (MS)
20 µm
7 (ACB, sh)
20 µm
8 (SHy)
ac
20 µm
9 (OT)
20 µm
10 (SCN)
opt
20 µm
11 (MnPO)
20 µm
12 (TMv, PMv, MBO)
MBO
TMv
20 µm
PMv
13 (RP3V)
50 µm
14 (RP3V)
20 µm
15 (VMN, Arc, TMv, PM, SUM, MBO)
PMd
SUM
VMH
DMH
PMv
MBO
TMv
500 µm
Arc
rostral
caudal
16 (Arc & VMH)
VMH
Arc
17 (ARC)
Kiss1r
Kiss1
Slc32a1
Slc17a6
18 (TMv)
19 (SUM & MBO)
SUM
MBO

739

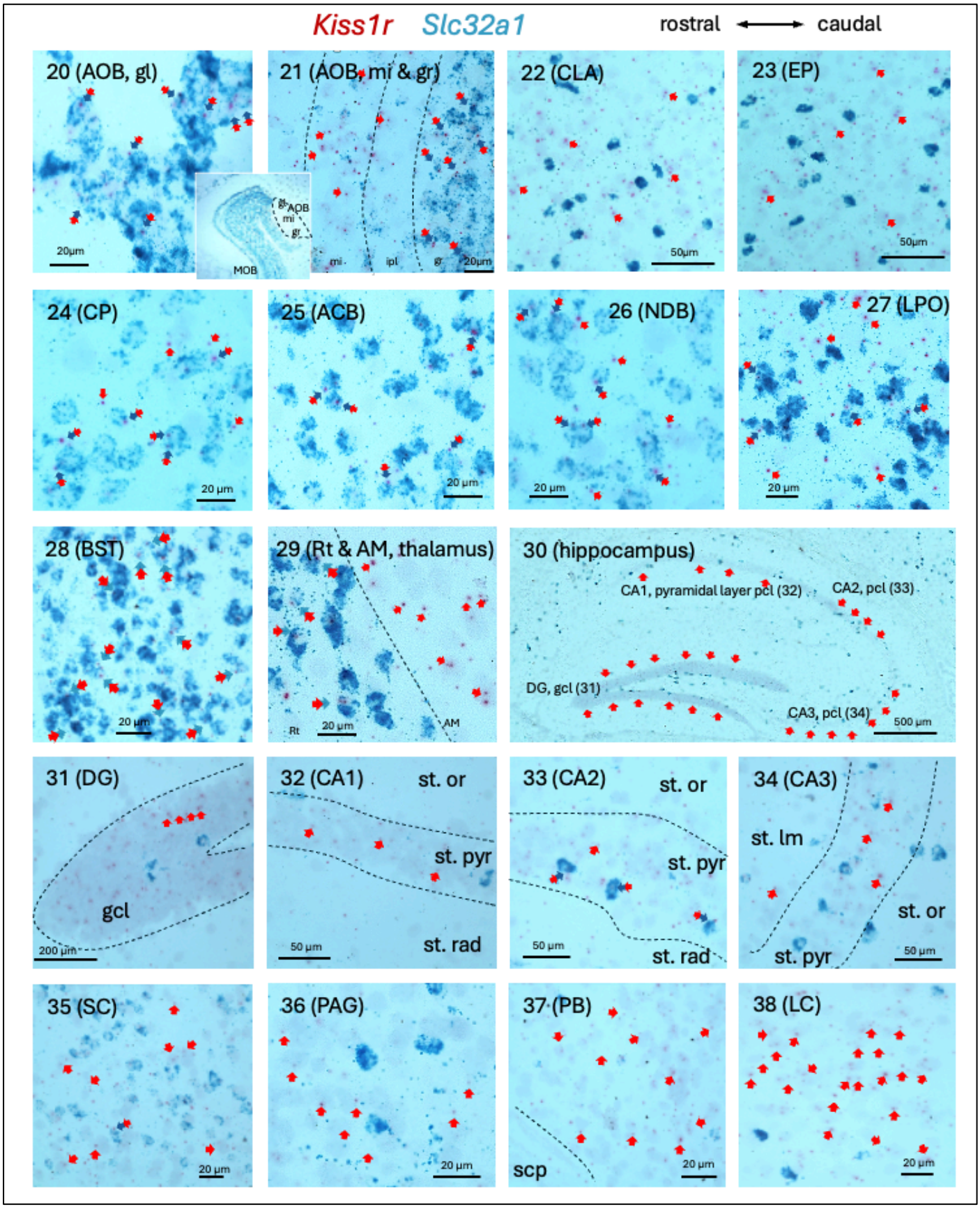
Kiss1r
Slc32a1
rostral
caudal
20 (AOB, gl)
21 (AOB, mi & gr)
22 (CLA)
23 (EP)
24 (CP)
25 (ACB)
26 (NDB)
27 (LPO)
28 (BST)
29 (Rt & AM, thalamus)
30 (hippocampus)
CA1, pyramidal layer pcl (32)
CA2, pcl (33)
DG, gcl (31)
CA3, pcl (34)
31 (DG)
gcl
32 (CA1)
st. or
st. pyr
st. rad
33 (CA2)
st. or
st. pyr
st. rad
34 (CA3)
st. lm
st. or
st. pyr
35 (SC)
36 (PAG)
37 (PB)
scp
38 (LC)

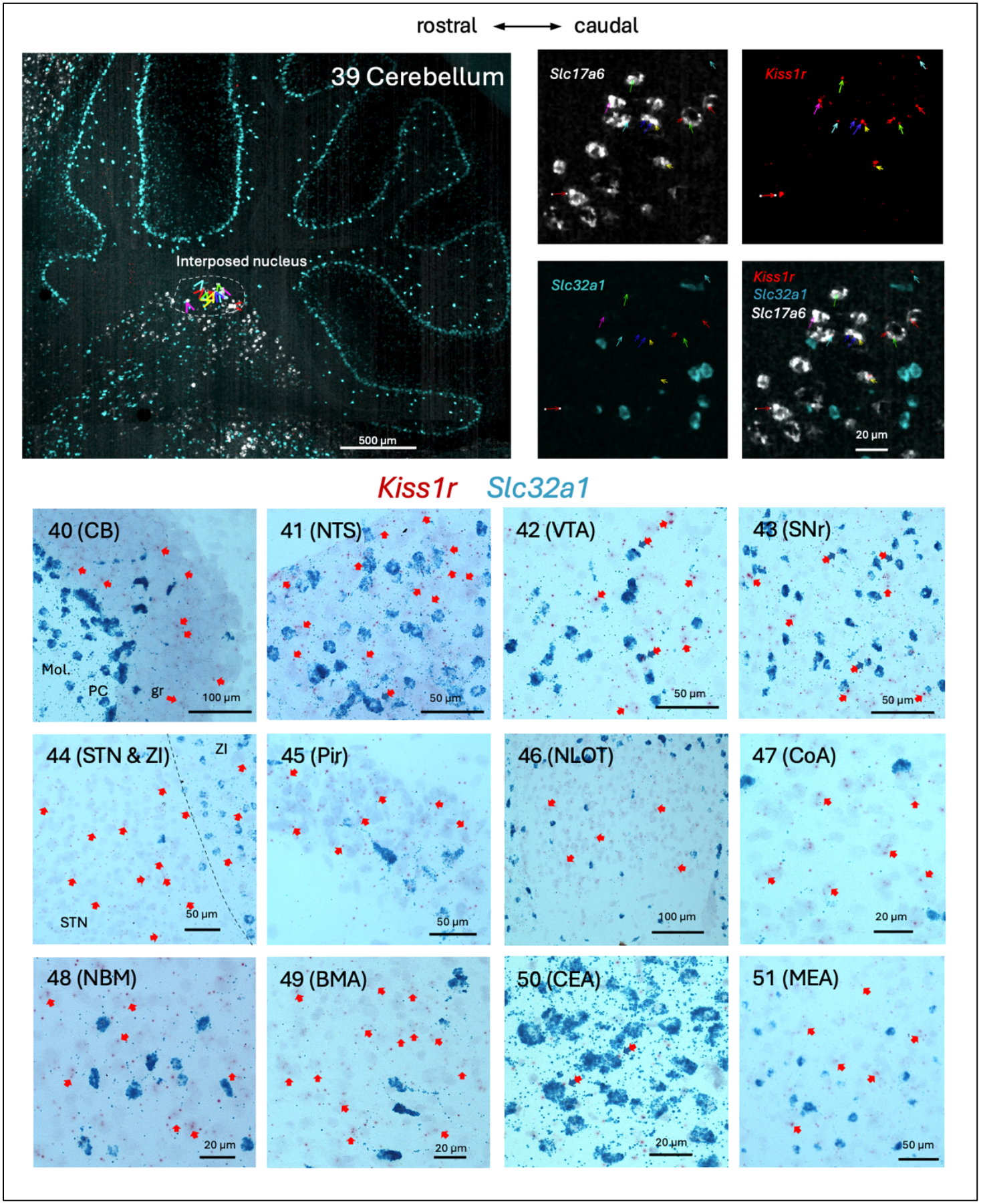
rostral
caudal
39 Cerebellum
Interposed nucleus
500 µm
Slc17a6
Kiss1r
Slc32a1
Kiss1r
Slc32a1
Slc17a6
20 µm
Kiss1r Slc32a1
40 (CB)
Mol.
PC
gr
100 µm
41 (NTS)
50 µm
42 (VTA)
50 µm
43 (SNr)
50 µm
44 (STN & ZI)
ZI
STN
50 µm
45 (Pir)
50 µm
46 (NLOT)
100 µm
47 (CoA)
20 µm
48 (NBM)
20 µm
49 (BMA)
20 µm
50 (CEA)
20 µm
51 (MEA)
50 µm

742

743 *Fig. 6* ***Examples illustrating Kiss1r co-expression with GABAergic neurons (Slc32a1 mRNA encoding***
744 ***VGAT) in cortical and subcortical regions from sagittal sections****.* ***Co-expression Kiss1r with Kiss1***
745 ***(mRNA encoding kisspeptin), Slc17a6 (mRNA encoding VGluT2) and Sla32a1, was examined at the***
746 ***RP3V and Arc regions (panels 14,17, and 39)****. Panels* ***1*** *and* ***2****: MOB, main olfactory bulb; gl, glomerular*
747 *layer; opl, outer plexiform layer; mi, mitral cell layer; ipl, inner plexiform layer; gr, granule cell layer.*
748 *N.B. Kiss1r (red dots) is widely expressed in the MOB periglomerular cells which are inhibitory*
749 *interneurons (Slc32a1, blue patches, co-expressing, bicolor arrows in panel 1). Kiss1r is also widely*
750 *expressed in the opl, not Slc32a1 expressing cells (red arrows) (panel 1). The principal projection cells*
751 *in MOB, the mitral cells, mi, are strongly expressing the Kiss1r (panel 2), as well as the GABAergic*
752 *neurons in the granule cell layer (gr). Panel* ***3****: PL, prelimbic area of prefrontal cortex (PfC), most Kiss1r*
753 *labeling (red arrows) are not on Slc32a1 expressing neurons. Panel* ***4****: somatosensorial cortex (SS Ctx),*
754 *layer 5-6, most Kiss1r labeling (red arrows) are not on Slc32a1 expressing neurons. In lateral, medial*
755 *septal nuclei (LS, panel* ***5****, and MS, panel* ***6****) and nucleus accumbens (ACB, panel 7), the Kiss1r was mainly*
756 *found in Slc32a1 expressing (GABAergic) neurons (bicolor double arrows). Panel* ***8****: Shy, septo-*
757 *hypothalamic nucleus, the Kiss1r labeling are main in none-Scl32a1 cells (red arrows). Panel* ***9*** *and* ***10****:*
758 *OT, olfactory tubercle and SCN, suprachiasmatic nucleus, the Kiss1r is almost exclusively expressed in*
759 *the Scl32a1 expressing neurons (bicolor double arrows). Panel* ***11****: MnPO, median preoptic nucleus,*
760 *Kiss1r is expressed in both GABAergic and no-GABAergic cells. In panel* ***12****, three adjacent hypothalamic*
761 *regions are displayed. TMv: tuberomammillary nucleus ventral division, most GABAergic neurons*
762 *expressed Kiss1; PMv, premammillary nucleus, ventral division, and MBO, mammillary body, almost all*
763 *the cells expressed Kiss1r on Slc32a1-negative cells. N.B. the wide and strong expression of Kiss1r in*
764 *PMv that almost every Nissl-stained nucleus contained Kiss1r strongly suggest that those kisspeptin*
765 *expressing neurons demonstrated in a recent report* [(1)] *use autocrine signaling mechanism. Panel* ***13****:*
766 *RP3V, rostro-periventricular n. of 3rd ventricle, where Kiss1r is widely expressed in both Slc32a1 positive*
767 *and negative cells. Panel* ***14****: examination of RP3V using 4 channels RNAscope LS Multiplex Fluorescent*
768 *Assay method against mRNA for kisspeptin receptor (Kiss1r, red dots), kisspeptin (Kiss1, green dots),*
769 *VGAT (Slc32a1, blue dots) and VGLUT2 (Slc17a6, white dots). Six out nine cells (6/9) in this confocal*
770 *microphotograph were found co-expressing the 4 mRNAs, indicated with quadri-color-arrows. Insets*
771 *show 4-channel separated screenshots of the cell in the center. The red thin arrows, generated by the*
772 *Leica Application Suite (LAS) software, indicate the very same coordinates in each channel and the*
773 *overlay. The three cells which were not Kiss1+ (not Slc32a1+) were all Slc17a6 (VGLUT2) expressing*
774 *as well as Kiss1r expressing. Panel* ***15****: low magnification micrograph showing relevant hypothalamic*
775 *nuclei regarding Kiss1r and Slc32a1 expression. VMN, ventromedial hypothalamic n., Arc, arcuate*
776 *hypothalamic n., TMv, tuberomammillary n. ventral division, PM, premammillary n. ventral and dorsal*
777 *divisions, SUM, supramammillary n., MBO, mammillary body. Panel* ***16****: Kiss1r in ventromedial*
778 *hypothalamic n. (VMH) is widely and exclusively expressed in no-Slc32a1 cells. In contrast, in the arcuate*
779 *hypothalamic n. (Arc), the Kiss1r is expressed in both Slc32a1 expressing cells (bicolor arrows) and cells*
780 *which do not express Slc32a1. Panel* ***17****: examination of Arc using 4 channels RNAscope LS Multiplex*
781 *Fluorescent Assay against mRNA for kisspeptin receptor (Kiss1r, red dots), kisspeptin (Kiss1, green dots),*
782 *VGAT (Slc32a1, blue dots) and VGLUT2 (Slc17a6 white dots). One out of three (1/3) cells in this confocal*
783 *microphotograph was found co-expressing the mRNAs for Kiss1r, and Slc17a6 Kiss1 expressing but not*
784 *the Slc32a1 (indicated with tricolor arrows). Insets show 4-channel separated screenshots of the cell in*
785 *the center. The red thin arrows, generated by the Leica Application Suite (LAS) software, indicate the*

786 *very same coordinates in each channel. Panel **18**: TMv, tuberomammillary n. ventral division: Kiss1r is*
787 *expressed in both Slc23a1, and no-Slc32a1 cells. Panel **19**: Kiss1r is strongly expressed in MBO as*
788 *already shown in panel 12 but weakly expressed in the supramammillary n. (SUM). Panels **20** and **21**:*
789 *Kiss1r expression in accessory olfactory bulb (AOB) with similar patterns of MOB (see panels 1 and 2),*
790 *i.e., strongly co-expressed with Slc32a1 (VGAT expressing cells) in periglomerular cells in gl. and granule*
791 *cells. In the projection layer (mi), the mitral cells which do not express Slc32a, also strongly expressed*
792 *Kiss1r. The AOB is primarily involved in processing pheromonal signals detected by the vomeronasal*
793 *organ (VNO) and is critical for mediating social and reproductive behaviors. Panel **22** and **23**: claustrum*
794 *(CLA) and endopiriform n. (EP), Kiss1r is mainly expressed in no-Slc32a1 neurons. Kiss1r is mainly co-*
795 *expressed in Slc32a1 (VGAT expressing) neurons in caudoputamen (CP, panel **24**), nucleus accumbens*
796 *(ACB, panel **25**), nucleus of diagonal band (NDB**,** panel **26),** bed nucleus of stria terminalis (BST, panel*
797 ***28**) and reticular thalamic nucleus (Rt, panel **29**, left). Panel **27** shows the mixed expression of Kiss1r, in*
798 *both Slc32a1postive and negative cells in the lateral preoptic area (LPO). In thalamus, the Kiss1r is*
799 *widely expressed (panel **29**, right half). In the hippocampal formation, Kiss1r is strongly expressed in the*
800 *projection neurons (Panels **30, 31, 32, 33** and **34**). Panel **35** and **36**: midbrain superior colliculus (SC)*
801 *and periaqueductal grey (PAG), Kiss1r mainly expressed in no-Slc32a1 expressing cells. Panel **37** and*
802 ***38**: pontine parabrachial n. (PB) and locus coeruleus (LC), Kiss1r mainly expressed in no-Slc32a1*
803 *expressing cells. Panel **39**: examination of cerebellum using 4 channels RNAscope LS Multiplex*
804 *Fluorescent Assay against mRNA for kisspeptin (negative and not showing), kisspeptin receptor (Kiss1r,*
805 *red dots), VGAT (Slc32a1, light blue patches) and VGLUT2 (Slc17a6, white patches). Interposed nucleus*
806 *was found co-expressing the mRNAs for Kiss1r and Slc17a6 but not the Slc32a1. The multicolor arrows,*
807 *generated by the Leica Application Suite (LAS) software, indicate the very same coordinates in each*
808 *channel. Panel **40**: wide expression of Kiss1r in cerebellar granule cell layer (gr). Panel **41**: wide*
809 *expression of Kiss1r in the brainstem nucleus tractus solitarii (NTS). Panel **42**, **43** and **44**, midbrain*
810 *ventral tegmental area (VTA), substantia nigra reticulata (SNr), interbrain subthalamic nucleus (STN)*
811 *and zona incerta (ZI). In the regions 40-44, the Kiss1r is expressed almost exclusively in Slc32a1-negative*
812 *cells. Panel **45** shows the strong Kiss1r expression in pyramidal cell layer of the piriform cortex (Pir).*
813 *Panel **46, 47, 49** and **51**: nucleus of lateral olfactory tract (NLOT), cortico-amygdalar nucleus (CoA),*
814 *basomedial amygdala (BMA) and medial amygdala (MeA): Kiss1r is widely expressed in Slc32a1-*
815 *negative cells of these basal forebrain structures. Panel **48**: nucleus basalis of Meynert (NBM), a group*
816 *of cholinergic neurons located in the basal forebrain, widely expressed the Kiss1r. Panel **50**: CEA, central*
817 *amygdala, Kiss1r is mainly expressed in Slc32a1-postive cells. Scale bars: indicated for each micrograph.*
818 *-------*
819

Table 2. Distribution, cell types and strength of main ***Kiss1r* expressing cell groups** in mouse brain with comparison of co-expression of ***Slc32a1*** (VGAT)

Cell group / sub-field	Co-expressing Slc17a6 (VGAT)	NO Slc32a1 (VGAT)
Cerebrum: cortical plate		
Olfactory area		
Main Olfactory bulb (MOB)		
Granular cell layer (gr)	+++	+
Inner plexiform layer (ipl)	-	-
Mitral cell layer (mi)	+	+++
Outer plexiform layer (opl)	-	+
Glomerular layer (gl)	+++	+
Accessory olfactory bulb (AOB)	n/r	+
Mitral cell layer (mi)	+	+++
Glomerular layer (gl)	++++	+
Granular layer (gr)	++++	+
Ant olfactory n. (AON)	+	++
Taenia Tecta (TT)	+	++
Piriform area: Pir2	-	+++
Piriform area: Pir3	-	++
N. lat. olfactory tract (NLOT)	-	+++
Cortical amygdalar area (CoA)	-	+++
Hippocampal formation		
dorsal dentate gyrus, granule cells layer (gcl)	+	++++
dorsal hippocampus CA1, pyramidal cell layer (pcl))	+	++++
dorsal hippocampus CA2, pcl	+	++++
dorsal hippocampus CA3, pcl	+	++++
hilus	++	++
Subiculum	++	++
Isocortex		
Layer I	+	++
Layer II-II	+	++
Layer IV	+	++
Layer V	+	++
Layer VI	+	+++
Agranular insular cortex	+	++++
Somatomotor areas		
2ry motor area, layer 2-3:	+	++
2ry motor area layer 5:	+	+++
1ry motor area, layer 2-3	+	++
1ry motor area, layer 5	+	++
Agranular insular cortex	+	+++
Orbital frontal cortex (OFC)		
OFC 1	+	++
OFC 2/3	+	+++
OFC 5	+	+++
Prefrontal Cortex (PFC)		
Ant cingulate cortex (ACC):		
ACC 2/3:	+	+++
ACC 5:	++	+++
Prelimbic (PL)		
PL 2/3	+	+++
PL 5	++	+++
Infralimbic (IL)		
IL 2/3	++	+++
IL 5	++	+++
Prim somatosensory a. SSp,		
SSp 1	+	++
SSp 2/3	+	++
SSp 4 (mouth)	+	++
SSp 5	+	++
SSp 6a	+	+++
Gustatory areas (GU)	+	++
Auditory area	+	++
Visual area	+	++
Visceral area (VISC)	+	++
Temporal association area	+	+++
Ectorhinal area	+	+++
Perirhinal area	+	++
Retrosplenial area	+	+++
Post parietal association area	+	+++
Cortical subplate		
Claustrum	+	++
Endopiriform nucleus	+	++
Lateral amygdalar nucleus (LA)	+	+++
Post amygdalar nucleus (PA)	+	+++
Basomedial amygdala (BMA)	+	+++
Basolateral amygdala (BLA)	+	+++
Cerebral nuclei		
Striatum		
Caudado putamen	+++	+
Lateral septal nucleus (LS)	++	++
Septalhypothalamic nucleus (SHy)	+++	+++
Anterior amygdala area (AAA)	++	+
Central amygdalar nucleus (CEA)	++	+
Medial amygdalar nucleus (MEA)	++	+
Pallidum (basal forebrain)		
Medial Septal nucleus (MS)	++	++
Bed nucleus of stria terminalis (BNST)	++	++
Nucleus basalis of Meyner	+	+++
Globus pallidus	+	++
Substantia innominata (SI)	+	++
Nucleus of diagonal band of Broca (NDB)	+	++
Nucleus Accumbens	++	+
Brain stem, inter-brain		
Thalamus		
Somato-motor related		
Subparafacicular nucleus, magnocellular part	-	+++
Subparafacicular area	-	+++
Peripeduncular nucleus	-	+++
Medial geniculate complex	-	+++
Polymodal association cortex related		
Lat. posterior n. thal	-	+++
Post. limiting nucleus	-	+++
Suprageniculate n.	-	+++
Anterodorsal n.	-	+++
Anteromedial n.	-	++
Parataenial n.	-	++
Intermedial n.	-	+++
Laterodorsal n.	-	+++
Centrolateral n	-	+++
Intermediodorsal n.	-	+++
Mediodorsal n.	-	+++
Pariventricular n.	-	+++
Parateanial n.	-	+++
N. of reuniens[n2]	-	+++
Posterior pretectal n.	-	+++
Precommissural n.	-	+++
Reticular nucleus of the thalamus (Rt)	+++	-
Epithalamus		
Medial habenula	-	++++
Lateral habenula	+	++++
Hypothalamus		
Paraventricular n (PVN)	+	++
Arcuate Nucleus	+++	-
Suprachiasmatic nucleus	+++	+
Rostro-periventricular of the 3V (RP3V)	+++	++
Anterodorsal preoptic n.	++	++
Anteroventral n.	+++	++
Dorsomedial n.	+++	++
Median preoptic n.	++	++
Medial preoptic area	++	++
Vascular organ of lamina terminalis	-	-
Lateral preoptic area (LPO)	++	+
Anterior hyp. area (AH)	+++	+
Premammilary n. (PM)	-	+++++
Lateral mammillary n.	-	+++++
Medial mammillary n. (MM)	-	+++++
Supramammillary n.(SUM)	++	++
Median preoptic n. (MnPO)	+	+++
Lateral hyp. area (LH)	++	++
Subthalamic nucleus (STN)	-	+++++
Retrochiasmatic area	+++	++

820

Tuberomammilary nucleus (TM, magnocellular subnucleus MTu)	+++	+++
Zona incerta (ZI)	++	+
Ventromedial hyp. n (VMH)	-	+++++
Post. hypothalamic n.	+	+
Midbrain		
Superior colliculus, sensorial (SCS)	+	+++
Superior colliculus, motor (SCM)	+	++
Inf. Colliculus (IC)	++	++
N. of the brachium of IC (BIC)	+	+
Ventral tegmental area (VTA)	+	+++
Sustantia nigra reticulata	+	+++
Midbrain reticular n.	+	++
Periaqueductal gray	++	+++
Midbrain raphe nuclei	+	+++
Pedunculopontine n.	+	++
Dorsal n. raphe	++	++
Pons		
N. lateral lemniscus	+	+
Principal sensorial nucleus of trigeminal nerve	-	++
Koelliker-Fuse subnucleus	-	++
Parabrachial n. lateral div.	-	+++
Superior olivary comp (lat)	-	++
Tegmental reticular n.	++	+++
Dorsal tegmental n.	++	+++
Pontine gray	-	++++
Pontine central gray	++	+++
Supratrigeminal nucleus	++	++
Locus Coeruleus (state)	-	++++
Laterodorsal tegmental n.	++	+++
Pontine reticular n.	++	+++
Superior central n. raphe	++	++
Medulla		
N. tractus solitarii medial	+	+++
N. tractus solitarii lateral	+	+++
Hypoglossal (XII) n.	+	++
Dorsal motor n. of the Vagus nerve (X)	+	+++
Dorsal cochlear n.	-	++
Ventral cochlear n.	-	++
Spinal n. trigeminal	+	++
N. prepositus	-	+++
Facial motor n. (VII)	++	++
N. ambiguus	++	+++
Magnocellular reticular n.	++	+++
Spinal vestibular n.	+++	++
N. X	+	++
N. raphe magnus (state related)	+	+++
N. raphe pallidus (state related)	+	+++
N. raphe obscurus (state rel.)	+	+++
Cuneate n.	+	+
Inferior olivary	+	+++
Cerebellar cortex		
Purkinje's cells	-	-
Golgi's cells	+	-
Granule cells[n4]	-	++++
Cerebellar nuclei		
Interposed n.	+	+
Dentate n.	-	++
Fastigial n.	+	++

* Semiquantitative annotations are used here (the percentage of expressing cell/total Nissl stained nuclei: "-", not detectable; "+", weak (<20%); "++", low (40%-20%); "+++", moderate (60%-40%); "++++", intense (80%-60%); "+++++", very intense (>80%).
** Functional neuroanatomy order and annotations are based on Allen Institute Mouse Reference Atlas.

4. General discussion and conclusions

This report continues our recent work[1] in which we provided a chemotype of seven *Kiss1*-expressing neuronal populations in the mouse brain. Our current study focuses on the distribution and density of kisspeptin (KP)-immunoreactive (KP-ir) fibers and cell bodies throughout the brains of mice and rats, as well as the distribution of the Kiss1 receptor (*Kiss1r*) in correlation with GABAergic neurons throughout the mouse brain and kisspeptinergic neurons in the hypothalamus.

4.1 Prominent KP fiber distribution in sensorial and brain state control centers: ageing and sex steroids

Our anatomical observations regarding the regional distribution of KP-ir fibers and cells in young and aged mice, along with the effects of short- and long-term gonadectomy, underscore the broader roles of KP signaling beyond reproductive functions, potentially including its involvement in sensory processing, behavioral state control, and emotional regulation. Additionally, the lack of a significant age-related decline in KP immunoreactivity - contrary to what is observed in other neuropeptide systems - raises intriguing questions about its role in aging-related diseases such as cancer[68], and neurodegeneration[69], as well as the mechanisms underlying its stability[40].

Aging has been associated with reductions in the density or functionality of various neuropeptide systems, such as neuropeptide Y (NPY), pituitary adenylate cyclase-activating polypeptide (PACAP), and pro-opiomelanocortin (POMC)[70-72] often correlating with cognitive decline, disrupted behavioral states, and changes in physiological homeostasis. With regard to the kisspeptin (KP) system, contrasting effects of aging on KP expression have been documented. It has been reported through immunohistochemistry

(IHC) that in aged male and female rats, KNDy-ARC neurons reduce their expression of KP, dynorphin, and neurokinin B peptides[73]. In contrast, studies in monkeys and postmortem human tissue reveal that aging correlates with a significant increase in the size of KiSS-1 mRNA-expressing neurons, as well as an increase in the number of labeled cells and autoradiographic grains per neuron[74].

The distribution patterns we report here indicate that many hypothalamic and extrahypothalamic regions are innervated by kisspeptin as strongly as the classical hypothalamic regions known for regulating the hypothalamic-pituitary-gonadal (HPG) axis. These may serve both reproduction-related behavioral, as well as non-reproductive, functions. Indeed, many of these regions are critical for regulating brain states, including telencephalic cortical areas basal forebrain (diagonal band nucleus, accumbens nucleus, septohypothalamic nucleus, medial and lateral septal nuclei), diencephalic structures (thalamic regions which are crucial for cortical activation, arousal and control of awareness such as reuniens nucleus, paraventricular thalamic nucleus anterior[75], hypothalamic median preoptic nucleus, suprachiasmatic nucleus (SCN), complex of the bed nucleus of stria terminalis (BST) and nucleus basalis of Meynert (NBM), midbrain regions (periaqueductal grey, dorsal raphe nucleus, substantia nigra and ventral tegmental area), and metencephalic areas such as the raphe nuclei, reticular formation, and locus coeruleus (see section 3.2 for more focused discussion).

A highlight of this study is the analysis of brains from aged male and female mice gonadectomized early in the lifespan. Notably, the KP fiber density in 22 regions associated with reproductive and non-reproductive functions was found to be similar to, or even increased in, gonadectomized animals compared to controls, suggesting that the KP system remains functional even after reproductive senescence.

KP signaling modulates sexual and emotional brain processing in humans[43]. Ogawa et al. found that kisspeptin in the habenula of zebrafish plays a role in fear responses[12, 76], suggesting that it may facilitate the removal of fear, which is essential for maintaining reproductive capabilities under stress. Kisspeptin's influence on anxiety-related behaviors has also been documented in kisspeptin receptor-deleted male mice, indicating that kisspeptin signaling may play a role in facilitating the activity of anxiogenic neural circuits operative in the elevated plus maze test (EPM)[8].

The interaction between kisspeptin and other neuropeptides was suggested by the work of Stincic et al., in which inputs to PVN and DMH nuclei from presumptive ARC^{KP} and $R3PV^{KP}$ neurons were demonstrated by electrophysiology and optogenetics experiments, suggesting the interaction of the KP system with other neuropeptide systems involved in homeostatic and autonomic regulation[77]. Effects of ICV injection of KP-13 suggest that this peptide stimulates the HPA axis, induces hyperthermia, activates motor behavior and causes anxiety in rats[78].

We have reported in this study that a high density of KP fibers is present in areas related to pain sensorial processing, such as the principal sensorial trigeminal nucleus, the gelatinous layer of the trigeminus and in the periaqueductal gray. In the literature, only a few studies have investigated KP's role in the modulating of the perception of exteroceptive or interoceptive non-reproductive functions. It has been shown that KP-10 activates calcium signaling pathways in cultured dorsal root ganglion cells, suggesting a possible participation in pain modulation[79]. Other regions classically involved in sensorial

907 processing have moderate/dense innervation of KP fibers, *i.e.,* superior colliculus for visual processing;
908 the inferior colliculus and superior olive for audition; the parabrachial nucleus and nucleus of the solitary
909 tract (NTS or Sol) for gustatory processing; and the olfactory tubercle, nucleus of the olfactory tract and
910 medial amygdala for olfaction. To our knowledge, the effect of KP on the activity of these regions and its
911 effect on sensorial integration has yet to be examined.
912
913 **4.2 KP receptor distribution suggests potential autocrine, paracrine and neurotransmission modes**
914 **for KP signaling**
915
916 Our findings highlight the significant expression of the KP receptor (*Kiss1r*) in various brain regions
917 involved in sensory processing and state control, including the main and accessory olfactory bulbs, septal
918 nuclei, tuberomammillary nuclei, suprachiasmatic nucleus, locus coeruleus, hippocampal pyramidal and
919 granule cell layers, thalamic nuclei, cerebellar granule cell layer, and interposed nucleus. Additionally,
920 *Kiss1r* was expressed in *Kiss1*-expressing hypothalamic cells, indicating a potential autocrine/paracrine
921 role for the peptide, as discussed in detail in Section 3.4.
922
923 This expression pattern aligns with previous literature that identifies *Kiss1r* in the hippocampus,
924 particularly in the dentate gyrus—an area critical for learning and memory[30, 80]. Activation of *Kiss1r* in
925 the hippocampus has been shown to increase the amplitude of excitatory postsynaptic currents (EPSCs),
926 suggesting a potential mechanism by which kisspeptin may enhance synaptic plasticity[80]. In the habenula,
927 prominent expression of *Kiss1* and *Kiss1r* has been reported[26, 30, 31], implicating kisspeptin signaling in
928 emotional regulation as shown in the zebrafish where it has been linked to the inhibition of fear
929 responses[12]. Additionally, expressions of Kiss1r have been reported in the amygdala, a region pivotal for
930 processing emotions such as fear and anxiety[26, 31], and the septum, which is involved in reward and
931 reinforcement processes[30]. Electrophysiological recordings demonstrate that gonadotropin-releasing
932 hormone (GnRH) septal neurons exhibit robust excitatory responses to kisspeptin application [81].
933 Moreover, the thalamus, known as a relay center for sensory information, also expresses Kiss1r[26, 30]),
934 while reports indicate its presence in medullary and pontine brainstem regions[30, 82]. Kiss1r expression
935 has been reported in the medial amygdala (MeApd) of male rats, contributing to the facilitation of erectile
936 function[61]. Finally, the striatum and cortical regions have been also shown to express Kiss1r[26, 82]
937 however we found no studies investigating the potential role of KP signaling in these regions. Collectively,
938 these findings underscore the complex and diverse roles of Kiss1r throughout the brain, suggesting that
939 the kisspeptin signaling pathway may be instrumental in modulating a wide array of sensory and emotional
940 processes.
941
942 **4.3 Controversies and some consideration**
943
944 Rather dramatic down-regulation in mRNA for kisspeptin (*Kiss1)* expression in the RP3V and up-
945 regulation in the Arc region, in term of dendritic mRNA expression, after acute gonadectomy and a
946 generally stronger Kiss1 expression in female mice vs males was recently reported [1], in agreement with
947 most of the previous reports characterizing KP mRNA expression in this region in both intact and
948 gonadactomized male and female rodents[83-86]. However, altered KP expression at the level of the nerve
949 terminal is more difficult to discern, perhaps because immunohistochemical terminal field appearance in

a given brain area is determined by the composite projections from multiple KP cell groups. In SI Figure 2, we analyzed the experiments from Allen Mouse Brain Connectivity Atlas open source to demonstrate the reciprocal and convergent Kiss1 innervations in mouse brain of KP^{RP3V} and KP^{Arc} and in SI Figure 3 we presented this notion in diagram. It is our hope that future investigations will be directed towards more granular analysis of the individual contributions of each KP neuronal population to the nerve terminals within given brain areas.

Contribution statement

Conceptualization: LZ, VSH, MAZ, RPM, LEE; data curation: LZ, VSH, MAZ, ORHP; investigation: LZ, VSH, MAZ, ORHP, RHG; methodology: LZ, VSH, RHG; project administration: LZ, VH, LEE; resources: LZ, LEE, RPM, ICA, RHG; visualization LZ, VSH; writing – original draft: LZ, VH, LEE; review & editing: all the co-authors.

Acknowledgement

The research leading to these results received funding from the National Autonomous University of Mexico, under Grant Agreement UNAM-PAPIIT-IG200121(LZ), and UNAM-PAPIIT-IA202724 (ORHP); Mexican Nacional Council for Humanity, Science and Technology (CONAHCYT), under Grant Agreement CF-2023-243 (LZ), NIMH-IR, NIH, under Grant Agreement MH002386 (LEE). The investigators of this study have been supported by the following fellowships: sabbatical year fellowship from the PASPA program of the Dirección General de Personal Académico (DGAPA) of the Universidad Nacional Autónoma de México (UNAM) (LZ, VSH); Mexican CONAHCYT sabbatical fellowship (LZ) and Fulbright-García Robles Fellowship (VSH), for sabbatical research year in LEE's laboratory of NIMH, NIH; DGAPA-UNAM PREI program for a sabbatical research stay (RPM) in LZ's lab in UNAM, Mexico. We thank Charles Gerfen, NIMH for his support and discussions about this study. We thank Mr. Jonathan Kuo and colleagues of the NIMH-IRP Systems Neuroscience Imaging Resource (SNIR, Director Ted Usdin) and Ms. Ivonne Sanchez Cervantes of the Microscopy Unit of the School of Medicine, UNAM for technical assistance.

References

1. Hernández VS, Zetter MA, Hernández-Pérez O, Hernández-González R, Camacho-Arroyo I, Millar RP, Eiden LE, Zhang L. A comprehensive chemotyping and gonadal regulation of seven kisspeptinergic neuronal populations in the mouse brain. *bioRxiv*. 20242024.07.23.604881.
2. Lee JH, Miele ME, Hicks DJ, Phillips KK, Trent JM, Weissman BE, Welch DR. KiSS-1, a novel human malignant melanoma metastasis-suppressor gene. *J Natl Cancer Inst*. 1996; **88**(23): 1731-7.
3. Pinilla L, Aguilar E, Dieguez C, Millar RP, Tena-Sempere M. Kisspeptins and reproduction: physiological roles and regulatory mechanisms. *Physiol Rev*. 2012; **92**(3): 1235-316.
4. Clarke H, Dhillo WS, Jayasena CN. Comprehensive Review on Kisspeptin and Its Role in Reproductive Disorders. *Endocrinol Metab (Seoul)*. 2015; **30**(2): 124-41.
5. Mills EGA, O'Byrne KT, Comninos AN. Kisspeptin as a Behavioral Hormone. *Semin Reprod Med*. 2019; **37**(2): 56-63.
6. Mills EG, Yang L, Abbara A, Dhillo WS, Comninos AN. Current Perspectives on Kisspeptins Role in Behaviour. *Front Endocrinol (Lausanne)*. 2022; **13**928143.
7. Stephens SBZ, Kauffman AS. Regulation and Possible Functions of Kisspeptin in the Medial Amygdala. *Front Endocrinol (Lausanne)*. 2017; **8**191.

995 8. Delmas S, Porteous R, Bergin DH, Herbison AE. Altered aspects of anxiety-related behavior in
996 kisspeptin receptor-deleted male mice. *Sci Rep*. 2018; **8**(1): 2794.
997 9. Ebrahimi Khonacha S, Janahmadi M, Motamedi F. Kisspeptin-13 Improves Spatial Memory
998 Consolidation and Retrieval against Amyloid-beta Pathology. *Iran J Pharm Res*. 2019; **18**(Suppl1): 169-
999 81.
000 10. Abdul Satar NM, Ogawa S, Parhar IS. Kisspeptin-1 regulates forebrain dopaminergic neurons in
001 the zebrafish. *Sci Rep*. 2020; **10**(1): 19361.
002 11. Sivalingam M, Ogawa S, Parhar IS. Habenula kisspeptin retrieves morphine impaired fear
003 memory in zebrafish. *Sci Rep*. 2020; **10**(1): 19569.
004 12. Ogawa S, Nathan FM, Parhar IS. Habenular kisspeptin modulates fear in the zebrafish. *Proc Natl*
005 *Acad Sci U S A*. 2014; **111**(10): 3841-6.
006 13. Liu X, Herbison AE. Kisspeptin Regulation of Neuronal Activity throughout the Central Nervous
007 System. *Endocrinol Metab (Seoul)*. 2016; **31**(2): 193-205.
008 14. Clarkson J, d'Anglemont de Tassigny X, Colledge WH, Caraty A, Herbison AE. Distribution of
009 kisspeptin neurones in the adult female mouse brain. *J Neuroendocrinol*. 2009; **21**(8): 673-82.
010 15. Muir AI, Chamberlain L, Elshourbagy NA, Michalovich D, Moore DJ, Calamari A, Szekeres PG,
011 Sarau HM, Chambers JK, Murdock P, Steplewski K, Shabon U, Miller JE, Middleton SE, Darker JG,
012 Larminie CG, Wilson S, Bergsma DJ, Emson P, Faull R, Philpott KL, Harrison DC. AXOR12, a novel human
013 G protein-coupled receptor, activated by the peptide KiSS-1. *J Biol Chem*. 2001; **276**(31): 28969-75.
014 16. Lehman MN, Hileman SM, Goodman RL. Neuroanatomy of the kisspeptin signaling system in
015 mammals: comparative and developmental aspects. *Adv Exp Med Biol*. 2013; **784**27-62.
016 17. Mikkelsen JD, Simonneaux V. The neuroanatomy of the kisspeptin system in the mammalian
017 brain. *Peptides*. 2009; **30**(1): 26-33.
018 18. Lehman MN, Coolen LM, Steiner RA, Neal-Perry G, Wang L, Moenter SM, Moore AM, Goodman
019 RL, Hwa-Yeo S, Padilla SL, Kauffman AS, Garcia J, Kelly MJ, Clarkson J, Radovick S, Babwah AV, Leon S,
020 Tena-Sempere M, Comninos A, Seminara S, Dhillo WS, Levine J, Terasawa E, Negron A, Herbison AE.
021 The 3(rd) World Conference on Kisspeptin, "Kisspeptin 2017: Brain and Beyond":Unresolved questions,
022 challenges and future directions for the field. *J Neuroendocrinol*. 2018e12600.
023 19. Zhang L, Hernandez VS. Synaptic innervation to rat hippocampus by vasopressin-immuno-
024 positive fibres from the hypothalamic supraoptic and paraventricular nuclei. *Neuroscience*. 2013;
025 **228**139-62.
026 20. Swanson LW. *Brain Architecture: Understanding the Basic Plan* Oxford, UK: Oxford University
027 Press, 2011.
028 21. Lee SH, Dan Y. Neuromodulation of brain states. *Neuron*. 2012; **76**(1): 209-22.
029 22. Zagha E, McCormick DA. Neural control of brain state. *Curr Opin Neurobiol*. 2014; **29**178-86.
030 23. Rosazza C, Minati L. Resting-state brain networks: literature review and clinical applications.
031 *Neurol Sci*. 2011; **32**(5): 773-85.
032 24. McCormick DA, Nestvogel DB, He BJ. Neuromodulation of Brain State and Behavior. *Annu Rev*
033 *Neurosci*. 2020; **43**391-415.
034 25. Berridge CW, Waterhouse BD. The locus coeruleus–noradrenergic system: modulation of
035 behavioral state and state-dependent cognitive processes. *Brain research reviews*. 2003; **42**(1): 33-84.
036 26. Lee DK, Nguyen T, O'Neill GP, Cheng R, Liu Y, Howard AD, Coulombe N, Tan CP, Tang-Nguyen
037 AT, George SR, O'Dowd BF. Discovery of a receptor related to the galanin receptors. *FEBS Lett*. 1999;
038 **446**(1): 103-7.
039 27. Franssen D, Tena-Sempere M. The kisspeptin receptor: A key G-protein-coupled receptor in the
040 control of the reproductive axis. *Best Pract Res Clin Endocrinol Metab*. 2018; **32**(2): 107-23.

041 28. Irwig MS, Fraley GS, Smith JT, Acohido BV, Popa SM, Cunningham MJ, Gottsch ML, Clifton DK,
042 Steiner RA. Kisspeptin activation of gonadotropin releasing hormone neurons and regulation of KiSS-1
043 mRNA in the male rat. *Neuroendocrinology*. 2004; **80**(4): 264-72.
044 29. Ringel MD, Hardy E, Bernet VJ, Burch HB, Schuppert F, Burman KD, Saji M. Metastin receptor is
045 overexpressed in papillary thyroid cancer and activates MAP kinase in thyroid cancer cells. *J Clin*
046 *Endocrinol Metab*. 2002; **87**(5): 2399.
047 30. Herbison AE, de Tassigny X, Doran J, Colledge WH. Distribution and postnatal development of
048 Gpr54 gene expression in mouse brain and gonadotropin-releasing hormone neurons. *Endocrinology*.
049 2010; **151**(1): 312-21.
050 31. Higo S, Honda S, Iijima N, Ozawa H. Mapping of Kisspeptin Receptor mRNA in the Whole Rat
051 Brain and its Co-Localisation with Oxytocin in the Paraventricular Nucleus. *J Neuroendocrinol*. 2016;
052 **28**(4).
053 32. Stout Steele M, Bennett RA. Clinical Technique: Dorsal Ovariectomy in Rodents. *Journal of*
054 *Exotic Pet Medicine*. 2011; **20**(3): 222-6.
055 33. Sophocleous A, Idris AI. Ovariectomy/Orchiectomy in Rodents. In: Idris AI, ed. *Bone Research*
056 *Protocols*. New York, NY: Springer New York 2019: 261-7.
057 34. Dhillo WS, Chaudhri OB, Patterson M, Thompson EL, Murphy KG, Badman MK, McGowan BM,
058 Amber V, Patel S, Ghatei MA, Bloom SR. Kisspeptin-54 stimulates the hypothalamic-pituitary gonadal
059 axis in human males. *J Clin Endocrinol Metab*. 2005; **90**(12): 6609-15.
060 35. Paxinos G, Franklin KBJ. *Paxinos and Franklin's the Mouse Brain in Stereotaxic Coordinates*
061 Elsevier Science, 2012.
062 36. Paxinos G, Watson C. *The Rat Brain in Stereotaxic Coordinates* Elsevier Science, 2007.
063 37. Zhang L, Hernandez VS, Gerfen CR, Jiang SZ, Zavala L, Barrio RA, Eiden LE. Behavioral role of
064 PACAP signaling reflects its selective distribution in glutamatergic and GABAergic neuronal
065 subpopulations. *Elife*. 2021; **10**.
066 38. Zhang L, Hernandez VS, Zetter MA, Eiden LE. VGLUT-VGAT expression delineates functionally
067 specialised populations of vasopressin-containing neurones including a glutamatergic perforant path-
068 projecting cell group to the hippocampus in rat and mouse brain. *J Neuroendocrinol*. 2020; **32**(4):
069 e12831.
070 39. Brailoiu GC, Dun SL, Ohsawa M, Yin D, Yang J, Chang JK, Brailoiu E, Dun NJ. KiSS-1 expression
071 and metastin-like immunoreactivity in the rat brain. *J Comp Neurol*. 2005; **481**(3): 314-29.
072 40. Ketterson ED, Nolan V, Jr. Adaptation, Exaptation, and Constraint: A Hormonal Perspective. *Am*
073 *Nat*. 1999; **154**(S1): S4-S25.
074 41. Risold PY, Swanson LW. Connections of the rat lateral septal complex. *Brain research Brain*
075 *research reviews*. 1997; **24**(2-3): 115-95.
076 42. Rizzi-Wise CA, Wang DV. Putting Together Pieces of the Lateral Septum: Multifaceted Functions
077 and Its Neural Pathways. *eNeuro*. 2021; **8**(6).
078 43. Comninos AN, Wall MB, Demetriou L, Shah AJ, Clarke SA, Narayanaswamy S, Nesbitt A, Izzi-
079 Engbeaya C, Prague JK, Abbara A, Ratnasabapathy R, Salem V, Nijher GM, Jayasena CN, Tanner M,
080 Bassett P, Mehta A, Rabiner EA, Honigsperger C, Silva MR, Brandtzaeg OK, Lundanes E, Wilson SR,
081 Brown RC, Thomas SA, Bloom SR, Dhillo WS. Kisspeptin modulates sexual and emotional brain
082 processing in humans. *J Clin Invest*. 2017; **127**(2): 709-19.
083 44. Sheehan TP, Chambers RA, Russell DS. Regulation of affect by the lateral septum: implications
084 for neuropsychiatry. *Brain research Brain research reviews*. 2004; **46**(1): 71-117.
085 45. Salib M, Joshi A, Katona L, Howarth M, Micklem BR, Somogyi P, Viney TJ. GABAergic Medial
086 Septal Neurons with Low-Rhythmic Firing Innervating the Dentate Gyrus and Hippocampal Area CA3. *J*
087 *Neurosci*. 2019; **39**(23): 4527-49.

088 46. Unal G, Crump MG, Viney TJ, Eltes T, Katona L, Klausberger T, Somogyi P. Spatio-temporal
089 specialization of GABAergic septo-hippocampal neurons for rhythmic network activity. *Brain Struct*
090 *Funct*. 2018; **223**(5): 2409-32.
091 47. Buzsaki G. Theta oscillations in the hippocampus. *Neuron*. 2002; **33**(3): 325-40.
092 48. Espinosa N, Caneo M, Alonso A, Moran C, Fuentealba P. Optogenetic stimulation of septal
093 somatostatin neurons disrupts locomotory behavior and regulates hippocampus cholinergic theta
094 oscillations. *bioRxiv*. 20222022.09.30.510330.
095 49. Shen L, Zhang GW, Tao C, Seo MB, Zhang NK, Huang JJ, Zhang LI, Tao HW. A bottom-up reward
096 pathway mediated by somatostatin neurons in the medial septum complex underlying appetitive
097 learning. *Nat Commun*. 2022; **13**(1): 1194.
098 50. Srividya R, Mallick HN, Kumar VM. The changes in thermal preference, sleep-wakefulness, body
099 temperature and locomotor activity in the rats with medial septal lesion. *Behav Brain Res*. 2005;
100 **164**(2): 147-55.
101 51. Tsanov M. Speed and Oscillations: Medial Septum Integration of Attention and Navigation.
102 *Front Syst Neurosci*. 2017; **11**67.
103 52. Joshi A, Salib M, Viney TJ, Dupret D, Somogyi P. Behavior-Dependent Activity and Synaptic
104 Organization of Septo-hippocampal GABAergic Neurons Selectively Targeting the Hippocampal CA3
105 Area. *Neuron*. 2017; **96**(6): 1342-57 e5.
106 53. Liu AKL, Lim EJ, Ahmed I, Chang RC, Pearce RKB, Gentleman SM. Review: Revisiting the human
107 cholinergic nucleus of the diagonal band of Broca. *Neuropathol Appl Neurobiol*. 2018; **44**(7): 647-62.
108 54. Dudek SM, Alexander GM, Farris S. Rediscovering area CA2: unique properties and functions.
109 *Nature reviews Neuroscience*. 2016; **17**(2): 89-102.
110 55. Semba K, Fibiger HC. Organization of central cholinergic systems. *Prog Brain Res*. 1989; **79**37-
111 63.
112 56. Floresco SB. The nucleus accumbens: an interface between cognition, emotion, and action.
113 *Annu Rev Psychol*. 2015; **66**25-52.
114 57. Riaz S, Puveendrakumaran P, Khan D, Yoon S, Hamel L, Ito R. Prelimbic and infralimbic cortical
115 inactivations attenuate contextually driven discriminative responding for reward. *Sci Rep*. 2019; **9**(1):
116 3982.
117 58. Capuzzo G, Floresco SB. Prelimbic and Infralimbic Prefrontal Regulation of Active and Inhibitory
118 Avoidance and Reward-Seeking. *J Neurosci*. 2020; **40**(24): 4773-87.
119 59. de Lima MAX, Baldo MVC, Oliveira FA, Canteras NS. The anterior cingulate cortex and its role in
120 controlling contextual fear memory to predatory threats. *Elife*. 2022; **11**.
121 60. Kataoka N, Shima Y, Nakajima K, Nakamura K. A central master driver of psychosocial stress
122 responses in the rat. *Science*. 2020; **367**(6482): 1105-12.
123 61. Gresham R, Li S, Adekunbi DA, Hu M, Li XF, O'Byrne KT. Kisspeptin in the medial amygdala and
124 sexual behavior in male rats. *Neurosci Lett*. 2016; **627**13-7.
125 62. Pineda R, Plaisier F, Millar RP, Ludwig M. Amygdala Kisspeptin Neurons: Putative Mediators of
126 Olfactory Control of the Gonadotropic Axis. *Neuroendocrinology*. 2017; **104**(3): 223-38.
127 63. Kim J, Semaan SJ, Clifton DK, Steiner RA, Dhamija S, Kauffman AS. Regulation of Kiss1
128 expression by sex steroids in the amygdala of the rat and mouse. *Endocrinology*. 2011; **152**(5): 2020-
129 30.
130 64. Dubois SL, Acosta-Martinez M, DeJoseph MR, Wolfe A, Radovick S, Boehm U, Urban JH, Levine
131 JE. Positive, but not negative feedback actions of estradiol in adult female mice require estrogen
132 receptor alpha in kisspeptin neurons. *Endocrinology*. 2015; **156**(3): 1111-20.

65. Rance NE. Menopause and the human hypothalamus: evidence for the role of kisspeptin/neurokinin B neurons in the regulation of estrogen negative feedback. *Peptides*. 2009; **30**(1): 111-22.
66. Starrett JR, Moenter SM. Hypothalamic kisspeptin neurons as potential mediators of estradiol negative and positive feedback. *Peptides*. 2023; **163**170963.
67. Goodman RL, Moore AM, Onslow K, Hileman SM, Hardy SL, Bowdridge EC, Walters BA, Agus S, Griesgraber MJ, Aerts EG, Lehman MN, Coolen LM. Lesions of KNDy and Kiss1R Neurons in the Arcuate Nucleus Produce Different Effects on LH Pulse Patterns in Female Sheep. *Endocrinology*. 2023; **164**(11).
68. Kim TH, Yoon JH, Cho SG. Kisspeptin Promotes Glioblastoma Cell Invasiveness Via the Gq-PLC-PKC Pathway. *Anticancer Res*. 2020; **40**(1): 213-20.
69. Sinen O, Sinen AG, Derin N, Aslan MA. Nasal application of kisspeptin-54 mitigates motor deficits by reducing nigrostriatal dopamine loss in hemiparkinsonian rats. *Behav Brain Res*. 2024; **468**115035.
70. Klinger K, Del Angel M, Caliskan G, Stork O. Increasing NPYergic transmission in the hippocampus rescues aging-related deficits of long-term potentiation in the mouse dentate gyrus. *Front Aging Neurosci*. 2023; **15**1283581.
71. Reglodi D, Atlasz T, Szabo E, Jungling A, Tamas A, Juhasz T, Fulop BD, Bardosi A. PACAP deficiency as a model of aging. *Geroscience*. 2018; **40**(5-6): 437-52.
72. Kappeler L, Gourdji D, Zizzari P, Bluet-Pajot MT, Epelbaum J. Age-associated changes in hypothalamic and pituitary neuroendocrine gene expression in the rat. *J Neuroendocrinol*. 2003; **15**(6): 592-601.
73. Kunimura Y, Iwata K, Ishigami A, Ozawa H. Age-related alterations in hypothalamic kisspeptin, neurokinin B, and dynorphin neurons and in pulsatile LH release in female and male rats. *Neurobiol Aging*. 2017; **50**30-8.
74. Rometo AM, Krajewski SJ, Voytko ML, Rance NE. Hypertrophy and increased kisspeptin gene expression in the hypothalamic infundibular nucleus of postmenopausal women and ovariectomized monkeys. *J Clin Endocrinol Metab*. 2007; **92**(7): 2744-50.
75. Biesbroek JM, Verhagen MG, van der Stigchel S, Biessels GJ. When the central integrator disintegrates: A review of the role of the thalamus in cognition and dementia. *Alzheimers Dement*. 2024; **20**(3): 2209-22.
76. Ogawa S, Parhar IS. Functions of habenula in reproduction and socio-reproductive behaviours. *Front Neuroendocrinol*. 2022; **64**100964.
77. Stincic TL, Qiu J, Connors AM, Kelly MJ, Ronnekleiv OK. Arcuate and Preoptic Kisspeptin Neurons Exhibit Differential Projections to Hypothalamic Nuclei and Exert Opposite Postsynaptic Effects on Hypothalamic Paraventricular and Dorsomedial Nuclei in the Female Mouse. *eNeuro*. 2021; **8**(4).
78. Csabafi K, Jaszberenyi M, Bagosi Z, Liptak N, Telegdy G. Effects of kisspeptin-13 on the hypothalamic-pituitary-adrenal axis, thermoregulation, anxiety and locomotor activity in rats. *Behav Brain Res*. 2013; **241**56-61.
79. Kelestimur H, Bulut F, Canpolat S, Ozcan M, Ayar A. Kisspeptin leads to calcium signaling in cultured rat dorsal root ganglion neurons. *Gen Physiol Biophys*. 2021; **40**(2): 155-60.
80. Arai AC. The role of kisspeptin and GPR54 in the hippocampus. *Peptides*. 2009; **30**(1): 16-25.
81. Dumalska I, Wu M, Morozova E, Liu R, van den Pol A, Alreja M. Excitatory effects of the puberty-initiating peptide kisspeptin and group I metabotropic glutamate receptor agonists differentiate two distinct subpopulations of gonadotropin-releasing hormone neurons. *J Neurosci*. 2008; **28**(32): 8003-13.

82. Mattam U, Talari NK, Thiriveedi VR, Fareed M, Velmurugan S, Mahadev K, Sepuri NBV. Aging reduces kisspeptin receptor (GPR54) expression levels in the hypothalamus and extra-hypothalamic brain regions. *Exp Ther Med*. 2021; **22**(3): 1019.
83. Smith JT, Cunningham MJ, Rissman EF, Clifton DK, Steiner RA. Regulation of Kiss1 gene expression in the brain of the female mouse. *Endocrinology*. 2005; **146**(9): 3686-92.
84. Smith JT, Dungan HM, Stoll EA, Gottsch ML, Braun RE, Eacker SM, Clifton DK, Steiner RA. Differential regulation of KiSS-1 mRNA expression by sex steroids in the brain of the male mouse. *Endocrinology*. 2005; **146**(7): 2976-84.
85. Kauffman AS. Gonadal and nongonadal regulation of sex differences in hypothalamic Kiss1 neurones. *J Neuroendocrinol*. 2010; **22**(7): 682-91.
86. Takumi K, Iijima N, Iwata K, Higo S, Ozawa H. The effects of gonadal steroid manipulation on the expression of Kiss1 mRNA in rat arcuate nucleus during postnatal development. *J Physiol Sci*. 2012; **62**(6): 453-60.
1.

194 ***Supplementary information (SI)***

195

196 Kisspeptin fiber and receptor distribution analysis suggests its 197 potential role in central sensorial processing and behavioral 198 state control

199

200 *Running title: Kiss1r and KP fiber mapping in rodent brain*

201

202

203 Limei Zhang[1,2,*c], Vito S. Hernández[1,2,*c], Mario A. Zetter[1,5], Oscar R. Hernández-Pérez[1], Rafael Hernández-
204 González[6], Ignacio Camacho-Arroyo[7], Lee E. Eiden[2,c], Robert P. Millar[1,3,4]

205

206 [1]Dept. Physiology, School of Medicine, National Autonomous University of Mexico, Mexico City, Mexico
207 [2]Section on Molecular Neuroscience, NIMH-IRP, NIH, Bethesda, MD, USA
208 [3]Centre for Neuroendocrinology, University of Pretoria
209 [4]Dept. of Integrative Biomedical Sciences, Institute of Infectious Disease and Molecular Medicine, University
210 of Cape Town, South Africa
211 [5]Department of Medicine and Health, University of La Salle, Mexico City, Mexico
212 [6]Vivarium, School of Medicine, National Autonomous University of Mexico, Mexico City, Mexico
213 [7]Research Unit in Human Reproduction, National Institute of Perinatology-Faculty of Chemistry, National
214 Autonomous University of Mexico, Mexico City, Mexico
215 [*]These authors share first authorship.
216 [c] Correspondence: limei@unam.mx, vitohdez@unam.mx, eidenl@mail.nih.gov

217

218 ***Supplementary Figures 1-3 and legends***

219

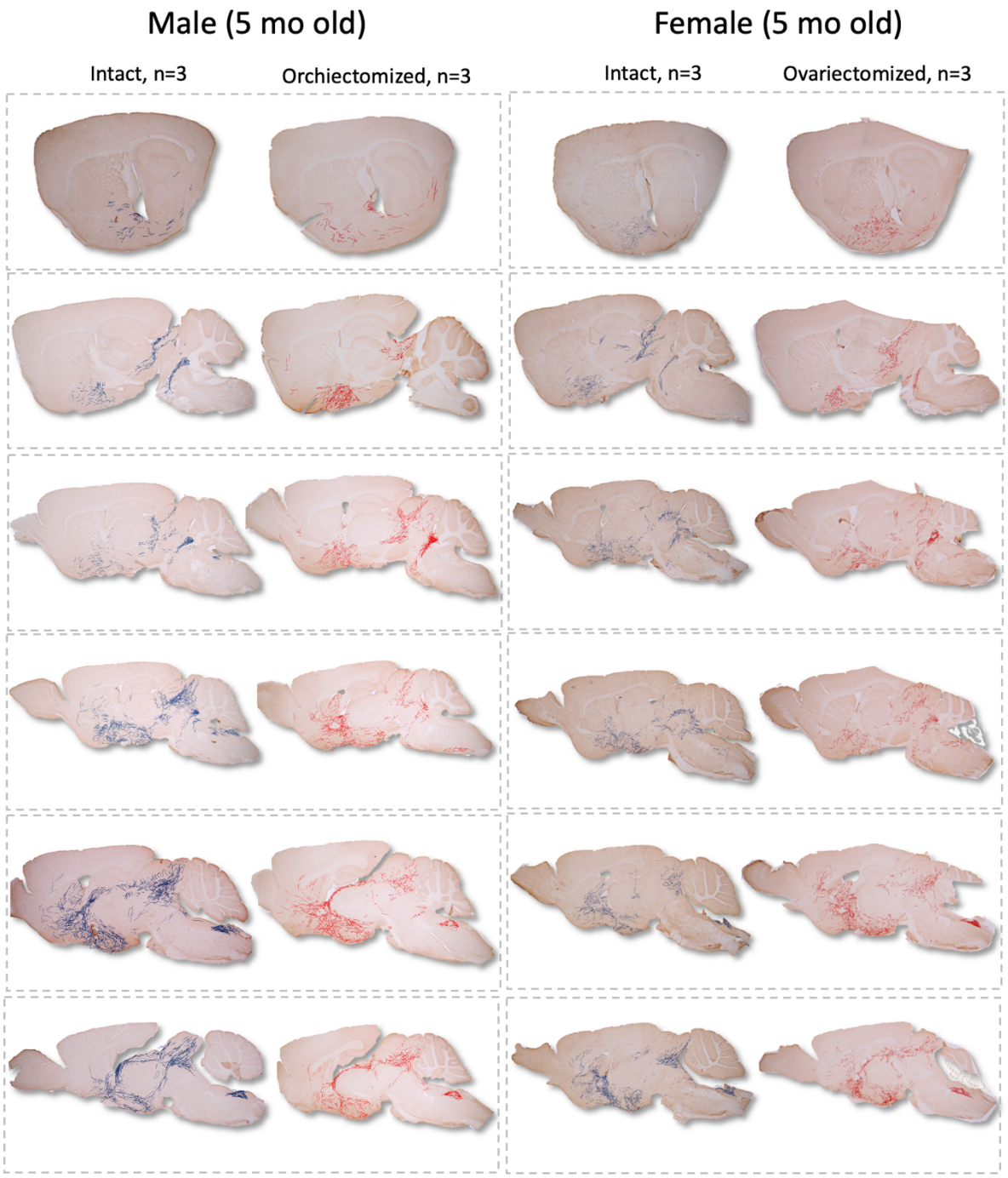

Supplementary Figure 1. *Comparison of cumulative (summed) fiber density charting of three young adult animals from each of the 4 experimental groups (male/female and intact/gonadectomized, N=12) represented in six different parasagittal levels. Hand-made drawings under microscope observations highlight the fiber distributions abstracted from the 3 subjects of the same group. Lines (control: blue, GNX, red) representing the KP-ir fibers which are "exaggerated" in term of thickness, in relation to the section area, for visualization sake.*

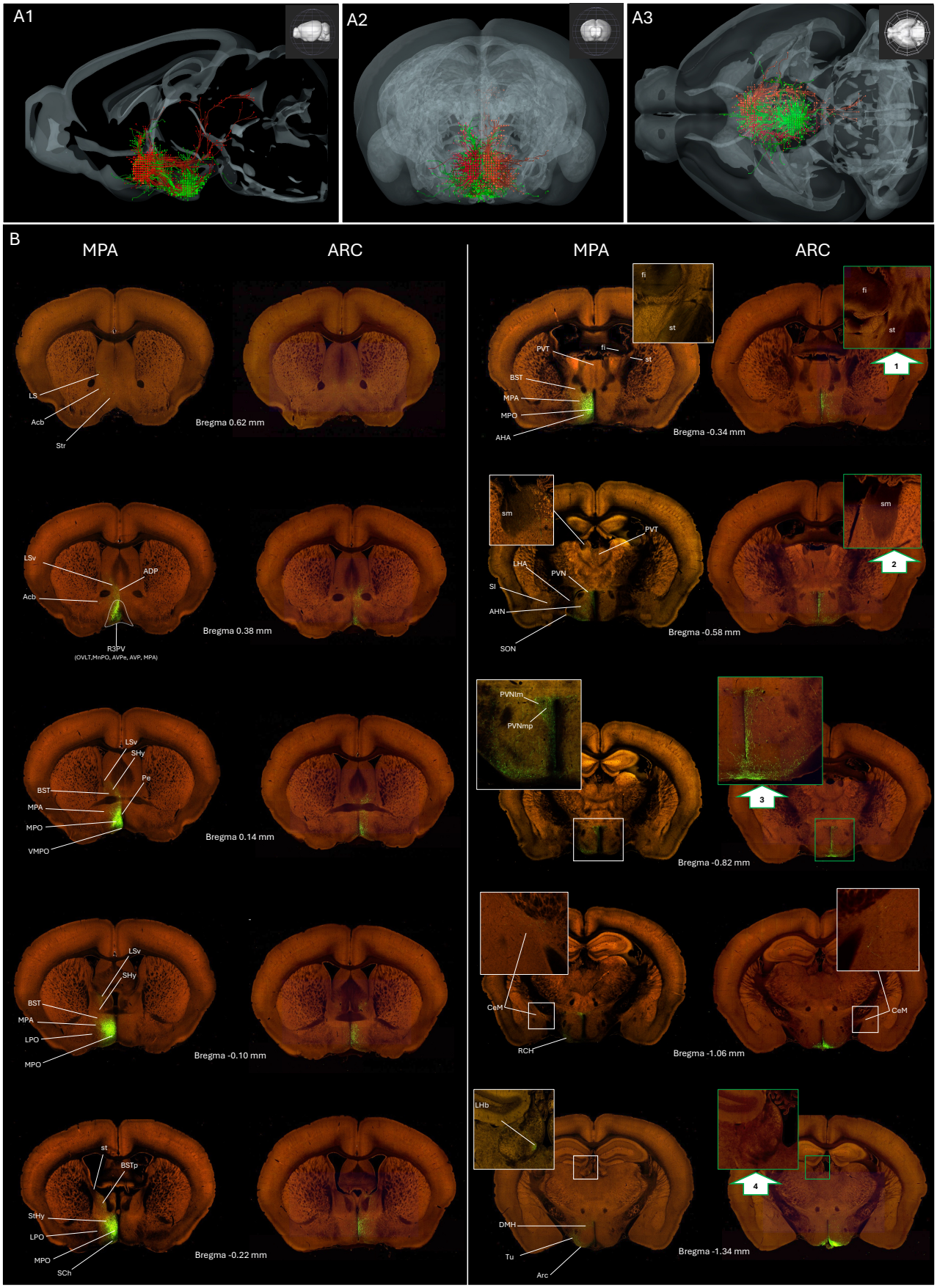
A1
A2
A3
B
MPA
ARC
MPA
ARC
LS
Acb
Str
Bregma 0.62 mm
LSv
ADP
Acb
R3PV
(OVLT,MnPO, AVPe, AVP, MPA)
Bregma 0.38 mm
LSv
SHy
Pe
BST
MPA
MPO
VMPO
Bregma 0.14 mm
LSv
SHy
BST
MPA
LPO
MPO
Bregma -0.10 mm
st
BSTp
StHy
LPO
MPO
SCh
Bregma -0.22 mm
fi
st
PVT
BST
MPA
MPO
AHA
Bregma -0.34 mm
1
sm
PVT
LHA
PVN
SI
AHN
SON
Bregma -0.58 mm
2
PVNlm
PVNmp
Bregma -0.82 mm
3
CeM
RCH
Bregma -1.06 mm
LHb
DMH
Tu
Arc
Bregma -1.34 mm
4

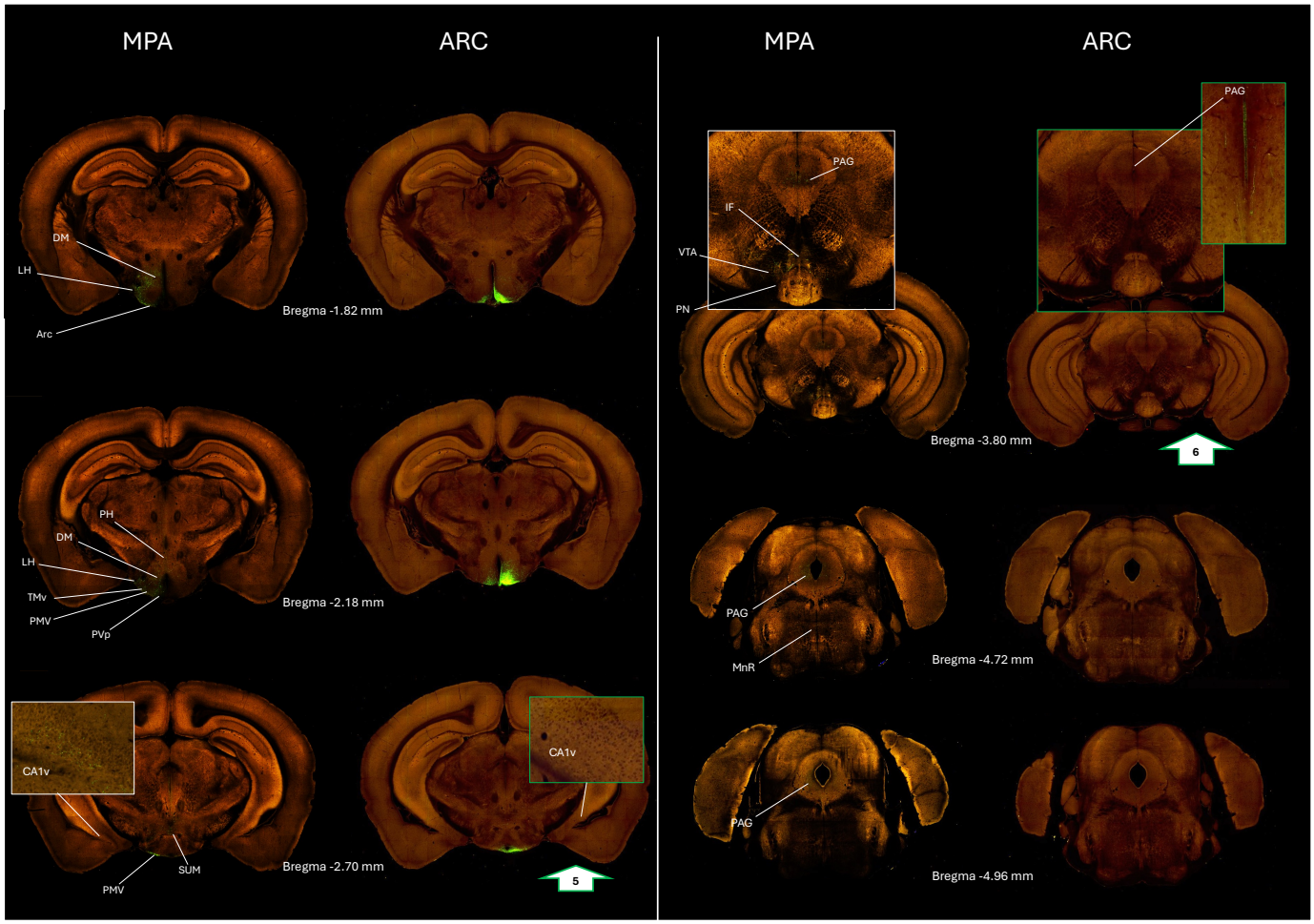

Supplementary Figure 2. Projection targets of R3PV or Arcuate Kiss1-Cre neurons transfected with AAV*. The data from two Kiss1-Cre mice injected in the arcuate nucleus (Arc, experiments 232311236 and 232310521) and two Kiss1-Cre mice injected in the rostral periventricular region (R3PV, experiments 299247009 and 301989585) injected with Cre-dependent tracer from the displayed in Allen Mouse Brain Connectivity Atlas this figure. Sagittal (A1), coronal (A2) and horizontal (A3) views of a 3-D representation with 3-D brain explorer of the innervation patterns of the two major populations of Kiss1 neurons. The VGAT-expressing R3PV neuronal population and its projections is represented in red, and the VGLUT2-expressing Arc population and its projections is represented in green. The different views show a reciprocal dense innervation between the Arc and the RP3V, additionally it is clear that the majority of regions in the striatum, septum, BNST, thalamus, hypothalamus, and amygdala, receive overlapping innervation from both regions. The ponto-mecencephalic region is mainly innervated by the R3PV. (B) Coronal sections at 17 rostro-caudal Bregma coordinates were selected from the animal that showed the best labelling for every level, for each level the left section from a R3PV injected mice was paired with a section from the Arc-injected mice. Some regions of interest are labelled in the RP3V sections, green-numbered arrows in the Arc sections indicate regions where there were differences in the innervation patterns between RP3V and Arc injected mice. Arrow #1: Some fibers were observed in the main stria terminalis and fimbria in the RP3V injected mice, but not in the Arc injected. Arrow #2: some fibers were observed in the stria medularis in the RP3v but not in the Arc injected mice. Arrow 3: The pattern of innervation of the paraventricular hypothalamic nucleus (PVN) is different between these experiments, the labelled axons of the mice injected in the RP3V innervate the magnocellular and parvocellular division, and the Arc injected neurons innervate preferentially the parvocellular region of the PVN. Also notice at this level and the following (Bregma -1.06) that for both injection targets, some*

axons travel laterally to reach the CeM. Arrow #4: the mice injected in the RP3V show innervation of the medial part of the lateral habenula (LHbm) specially the rostral part, thes fibers appear to travel via the stria medullaris (see arrow 2). No fibers in LHb were found in the Arc experiments. Arrow #5: A plexus of labelled fibers can be observed in the CA1 pyramidal layer of the ventral hippocampus, these fibers originate in the RP3V and travel trough the stria terminalis (see arrow 1). No fibers were found at this location in the Arc injected mice. Arrow #6: Fibers from the RP3V reach the mecencephalic region and innervate the periaquieductal gray region (PAG), the interfascicular nucleus (IF), the ventral tegmental area (VTA) and the median raphe (MnR). The mice injected in the Arc, show sparse axons and mainly innervate the PAG.

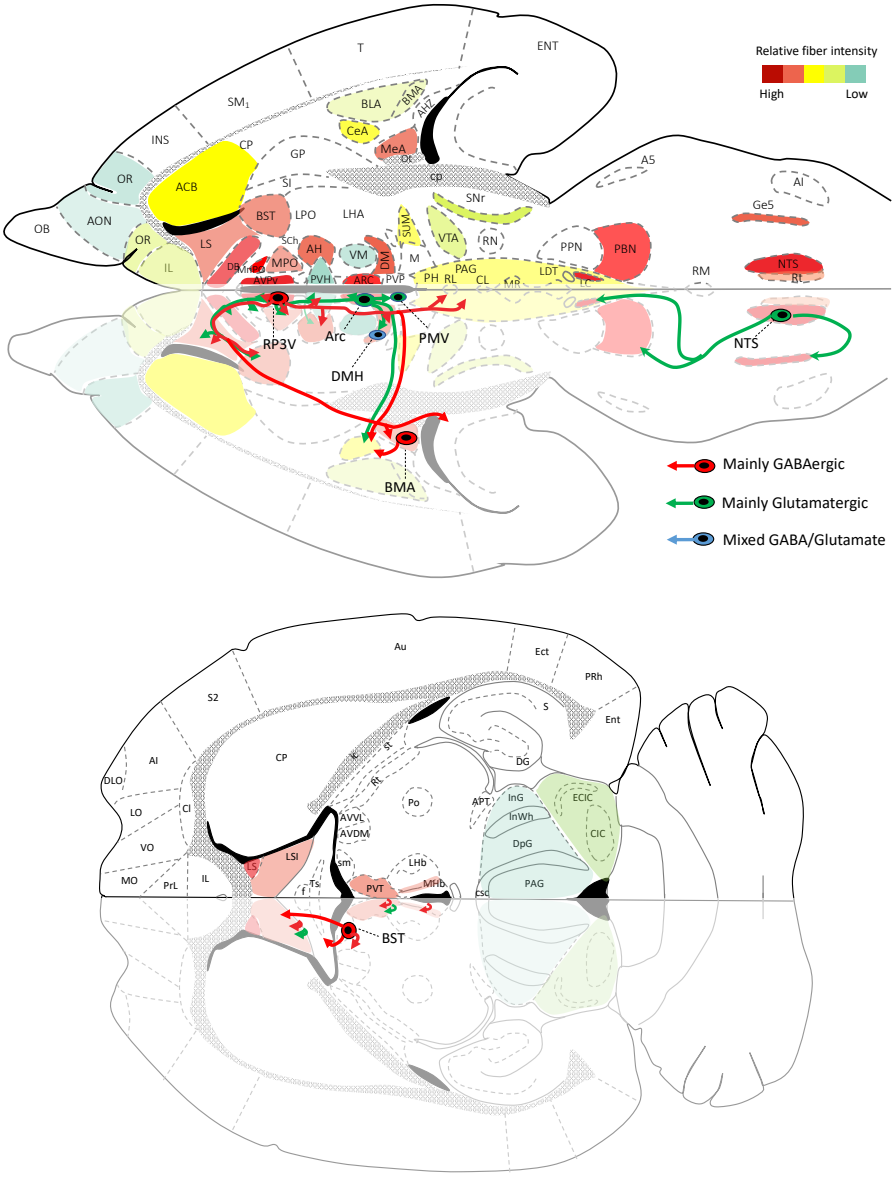

Supplementary Figure 3.. Kisspeptin fiber density Kisspeptin pathways to regions involved in brain state control, as well as motor and sensorial processing. *The density of kisspeptin observed through the brain of the "ideal mouse" i.e. the maximum density found in males or females through all gonadal states is represented as a relative fiber density, color coded in two horizontal levels of flatmap where some of the most innervated regions related to brain state, sensorial processing and motor integration were found. The bottom part of the drawing represent the pathways that we identified using analysis of several consecutive immunoreacted slices in different planes, as well as data obtained from four experiments published in the Allen brain atlas. the seven populations described in this report are labelled and shown in red if they are mainly Slc32A1 (VGAT) expressing or in green inf they are mainly Slc17a6 (VGLUT2) expressing. The population of the DMH was hosted GABAergic and Glutamatergic neurons and is coded in blue.*

2.